2007

Planning reactive power control for transmission enhancement

Haifeng Liu
Iowa State University

Planning reactive power control for transmission enhancement

by

Haifeng Liu

A dissertation submitted to the graduate faculty

in partial fulfillment of the requirements for the degree of

DOCTOR OF PHILOSOPHY

Major: Electrical Engineering

Program of Study Committee:
James D. McCalley, Major Professor
Venkataramana Ajjarapu
Nicola Elia
Chen-Ching Liu
Leigh Tesfatsion

Iowa State University

Ames, Iowa

2007

TABLE OF CONTENTS

LIST OF TABLES v

LIST OF FIGURES vi

ACKNOWLEDGEMENTS vii

ABSTRACT viii

CHAPTER 1 INTRODUCTION 1

1.1 Voltage Stability and Reactive Power Control 2

1.2 Reactive Power Control Planning 8

1.3 Dissertation Organization 15

CHAPTER 2 LINEAR COMPLEXITY SEARCH ALGORITHM TO LOCATE REACTIVE POWER CONTROL 17

2.1 Introduction 17

2.2 Voltage Stability Margin Sensitivity 17

2.3 Optimization Problem Formulation 20

2.4 Methodology 22

2.4.1 Overall Procedure 22

2.4.2 Backward Search Algorithm 27

2.4.3 Forward Search Algorithm 29

2.5 Case Study 29

2.5.1 Candidate Location Selection for Shunt Capacitors 31

2.5.2 Candidate Location Selection for Series Capacitors 36

2.6 Summary 38

CHAPTER 3 REACTIVE POWER CONTROL PLANNING TO RESTORE EQUILIBRIUM 39

3.1 Introduction 39

3.2 Contingency Analysis via Parameterization and Continuation 40

3.2.1 Parameterization of Branch Outage 40

3.2.2 Parameterization of HVDC Link Outage 42

3.2.3 Parameterization of Generator Outage 43

3.2.4 Continuation Method 44

3.3 Formulation for Reactive Power Control Planning 46

3.3.1 Flowchart for Reactive Power Control Planning 46

3.3.2 Voltage Stability Analysis 47

3.3.3 Selection of Candidate Control Locations 48

3.3.4 Formulation of Initial Mixed Integer Programming 48

3.3.5 Formulation of MIP with Updated Information 51

3.4 Application to New England System 52

3.5 Summary 56

CHAPTER 4 REACTIVE POWER CONTROL PLANNING TO INCREASE VOLTAGE STABILITY MARGIN 57

4.1 Introduction 57

4.2 Algorithm of Reactive Power Control Planning 58

4.2.1 Selection of Candidate Control Locations 59

4.2.2 Formulation of Initial Mixed Integer Programming 60

4.2.3 Formulation of MIP with Updated Information 63

4.3 Numerical Results 64

4.4 Summary 67

CHAPTER 5 OPTIMAL ALLOCATION OF STATIC AND DYNAMIC VAR RESOURCES 69

5.1 Introduction 69

5.2 Transient Voltage Sensitivities 70

5.2.1 Sensitivity of Voltage Dip Time Duration to SVC Capacitive Limit 72

5.2.2 Sensitivity of Maximum Transient Voltage Dip to SVC Capacitive Limit 73

5.2.3 Numerical Approximation 74

5.3 Algorithm of Optimal Allocation of Static and Dynamic VAR Resources 74

5.3.1 Contingency Analysis 75
5.3.2 Selection of Candidate VAR Locations 76
5.3.3 Formulation of Initial Mixed Integer Programming 76
5.3.4 Formulation of MIP with Updated Information 80
5.4 Numerical Results 82
5.5 Summary 87
CHAPTER 6 CONCLUSTIONS AND FUTURE WORK 88
6.1 Conclusions 88
6.2 Future Work 90
APPENDIX A HYBRID SYSTEM MODEL 92
APPENDIX B TRAJECTORY SENSITIVITIES 94
REFERENCES 96

LIST OF TABLES

Table 1.1 Capabilities of different reactive power control devices 7

Table 1.2 Cost comparison for reactive power control devices 8

Table 2.1 Base case loading and dispatch for the modified WECC system 30

Table 2.2 Voltage stability margin under contingencies for the WECC system 31

Table 2.3 Steps taken in the backward search algorithm for shunt capacitor planning 32

Table 2.4 Steps taken in forward search algorithm for shunt capacitor planning 34

Table 2.5 Steps taken in forward search algorithm for series capacitor planning 37

Table 3.1 Parameter values in the optimization formulation to restore equilibrium 54

Table 3.2 Critical point under two severe contingencies for the New England system 54

Table 3.3 Control allocations for shunt and series capacitors to restore equilibrium 55

Table 3.4 Critical point under planned controls 55

Table 4.1 Parameter values in the optimization formulation 65

Table 4.2 Voltage stability margin under three moderate contingencies 65

Table 4.3 Control allocations for shunt capacitors to increase voltage stability margin 67

Table 4.4 Control allocations for shunt and series capacitors to increase voltage stability margin 67

Table 4.5 Voltage stability margin under planned controls 67

Table 5.1 Parameter values adopted in optimization problem 82

Table 5.2 Contingencies violating reliability criteria 83

Table 5.3 Allocation of mechanically switched shunt capacitors 84

Table 5.4 Allocation of SVCs 84

Table 5.5 System performance under planned static and dynamic VARs 85

LIST OF FIGURES

Figure 1.1 Classification of power system stability 3

Figure 1.2 Voltage stability margin under different conditions 4

Figure 1.3 Voltage performance parameters for NREC/WECC planning standards. 6

Figure 1.4 Flowchart for reactive power control planning 14

Figure 2.1 Determination of expansion year 24

Figure 2.2 Flowchart for candidate control location selection 26

Figure 2.3 Graph for 4-switch problem 28

Figure 2.4 Modified WECC nine-bus system 30

Figure 2.5 Graph for the backward search algorithm for shunt capacitor planning 33

Figure 2.6 Graph for the forward search algorithm for shunt capacitor planning 34

Figure 2.7 Graph for the forward search algorithm for series capacitor planning 37

Figure 3.1 Parameterization of branch outage 41

Figure 3.2 Parameterization of HVDC link outage 43

Figure 3.3 Bifurcation curve obtained by the continuation method 45

Figure 3.4 Flowchart for the minimum reactive power control planning to restore equilibrium 47

Figure 3.5 New England 39-bus test system 53

Figure 4.1 Flowchart for the reactive power control planning to increase voltage stability margin 59

Figure 5.1 Static VAR compensator model 71

Figure 5.2 Slow voltage recovery after a fault 73

Figure 5.3 Flowchart for the static and dynamic VAR allocation 75

Figure 5.4 Voltage response at bus 7 under contingency 2 85

Figure 5.5 SVC output at bus 6 under contingency 2 86

Figure 5.6 SVC output at bus 7 under contingency 2 86

ACKNOWLEDGEMENTS

First, I would like to thank my advisor, Dr. James McCalley, for his support, patience, understanding, and encouragement during the whole work with this dissertation. His advice was essential to the completion of this work. He has taught me a number of valuable insights on conducting academic research in general.

I would like to thank the rest of my program of study committee: Dr. Venkataramana Ajjarapu, Dr. Nicola Elia, Dr. Chen-Ching Liu, and Dr. Leigh Tesfatsion. I greatly appreciate their valuable comments on this work as well as their other contributions as members of my committee. Thank you for all your advice to help me improve my work.

I am also indebted to the alumni and graduate students in the power system group at Iowa State University, Dr. Qiming Chen, Dr. Zhong Zhang, Dr. Wenzheng Qiu, Dr. Yong Jiang, Dr. Xiaoming Wang, Dr. Badri Ramanathan, Dr. Wei Shao, Dr. Qian Liu, Dr. Shu Liu, Yuan Li, Feng Gao, Fei Xiao, Sheng Yang, Gang Shen, Cheng Luo, Chee-Wooi Ten and many others. I am fortunate to have the opportunity to meet them and work with them. I appreciate all their friendships.

I would like to thank my mother and my father, for their endless support and encouragement in every one of my endeavors. Last but not least, I thank my wife, Licheng Jin, for the love and support she gave to me through all these years.

The author acknowledges the financial support of the National Science Foundation and the Office of Naval Research under the Electric Power Networks Efficiency and Security (EPNES) program, award ECS0323734, for this research work.

ABSTRACT

Sufficient controllable reactive power resources are essential for reliable operation of electric power systems. Inadequate reactive power support has led to voltage instability and has been a cause of several recent major power outages worldwide. Motivated by the industry need of effective algorithms of reactive power control planning to counteract voltage instability, this dissertation has developed a general framework for reactive power control planning to mitigate voltage instability and thus enhance the electric transmission system.

A backward/forward search algorithm with linear complexity is developed to select candidate locations of reactive power controls while satisfying power system performance requirements. A mixed integer programming based algorithm is presented for reactive power control planning to restore equilibria under severe contingencies. A mixed integer programming based algorithm of reactive power control planning is developed to increase post-contingency voltage stability margins. A systematic algorithm is developed to coordinate planning of static and dynamic reactive power control devices while satisfying the performance requirements of voltage stability margin and transient voltage dip. All the developed algorithms are implemented with MATLAB and tested on the New England 39-bus system. The simulation results obtained indicate that the developed approaches can be used to effectively plan reactive power control devices for transmission enhancement.

CHAPTER 1 INTRODUCTION

Future reliability levels of the electric transmission system require proper long-term planning to strengthen and expand transmission capability so as to accommodate expected transmission usage growth from normal load growth and increased long-distance power transactions. There are three basic options for strengthening and expanding transmission: (1) build new transmission lines, (2) build new generation at strategic locations, and (3) introduce additional control capability. Although all of these will continue to exist as options in the future, it is clear that options (1) and (2) have and will continue to become less and less viable. One obvious impediment to construction of new transmission is the need to acquire new right-of-way. This is not only expensive but also politically difficult due to environmental concerns as well as the public's inherent resistance to siting high voltage facilities close to home or work. The recent emphasis on managing (particularly maintaining) existing assets is a response to this trend. In addition, the disaggregation of the traditional regulated, monopolistic utility company into a multiplicity of generation, transmission, distribution, and power marketing companies hinders strategic siting of generation for purposes of transmission enhancement since generation and transmission are owned and operated by separate organizations.

As a result, there is significantly increased potential for application of additional power system control in order to strengthen and expand transmission in the face of growing transmission usage. The incentives for doing so are clear: there is little or no right-of-way, and relative to building new transmission or generation facilities, capital investment is much less.

Although considerable work has been done in planning transmission in the sense of options (1)-(2), there has been little effort towards planning transmission control options in the

sense of option (3), yet the ability to consider these devices in the planning process is a clear need to the industry [1, 2, 3, 4]. The capacity of electric transmission systems may be constrained by thermal limits, voltage magnitude limits, or stability limits. Reference [5] provides a summary of power system planning methods to relieve thermal overloads or voltage magnitude violations on transmission facilities. There is less work done in the field of power system control planning to enhance the transmission system constrained by stability problems.

The objective of this work is to design systematic control system planning algorithms to expand the capability of electric transmission systems with stability constraints. The proposed control planning algorithm will answer the following three questions:

- what type of control device is needed,
- where to implement the enhancement, and
- how much is the control device needed.

1.1 Voltage Stability and Reactive Power Control

In the IEEE/CIGRE report [6], power system stability can be classified into rotor angle stability, voltage stability, and frequency stability as shown in Figure 1.1:

- Rotor angle stability refers to the capability of synchronous machines in an interconnected power system to remain in synchronism subjected to a disturbance.
- Voltage stability refers to the capability of a power system for maintenance of steady voltages at all buses in the system subjected to a disturbance under given initial operating conditions.
- Frequency stability refers to the capability of a power system for maintenance of

steady frequency following a severe system upset resulting in a significant imbalance between generation and load.

All these stability problems can lead to system failure [7]. However, voltage instability has been a cause of several recent major power outages worldwide [7], [8]. In this work, we focus on systems only having the voltage stability problem. The proposed control planning approach can be extended to consider other stability/security problems as well.

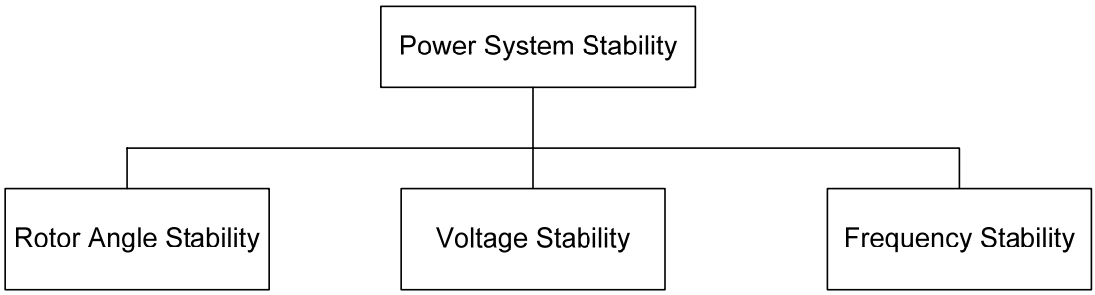

Figure 1.1 Classification of power system stability

Planning power systems is invariably performed under the assumption that the system is designed to withstand a certain set of contingencies. There is currently a disturbance-performance table within the NERC (North American Electric Reliability Corporation)/WECC (Western Electricity Coordinating Council) planning standards [9] which provides minimum post-disturbance performance specifications for credible events. The post-disturbance performance criteria regarding voltage stability include:

- Minimum post-contingency voltage stability margin,
- Transient voltage dip criteria (magnitude and duration).

The rest of this section will introduce voltage stability margin and transient voltage dip.

Voltage stability margin is defined as the amount of additional load in a specific pattern of load increase that would cause voltage instability as shown in Figure 1.2. The potential for contingencies such as unexpected component (generator, transformer, transmission line) outages in an electric power system often reduces the voltage stability margin [10], [24]. Note that severe contingencies may cause the voltage stability margin to be negative (i.e. voltage instability).

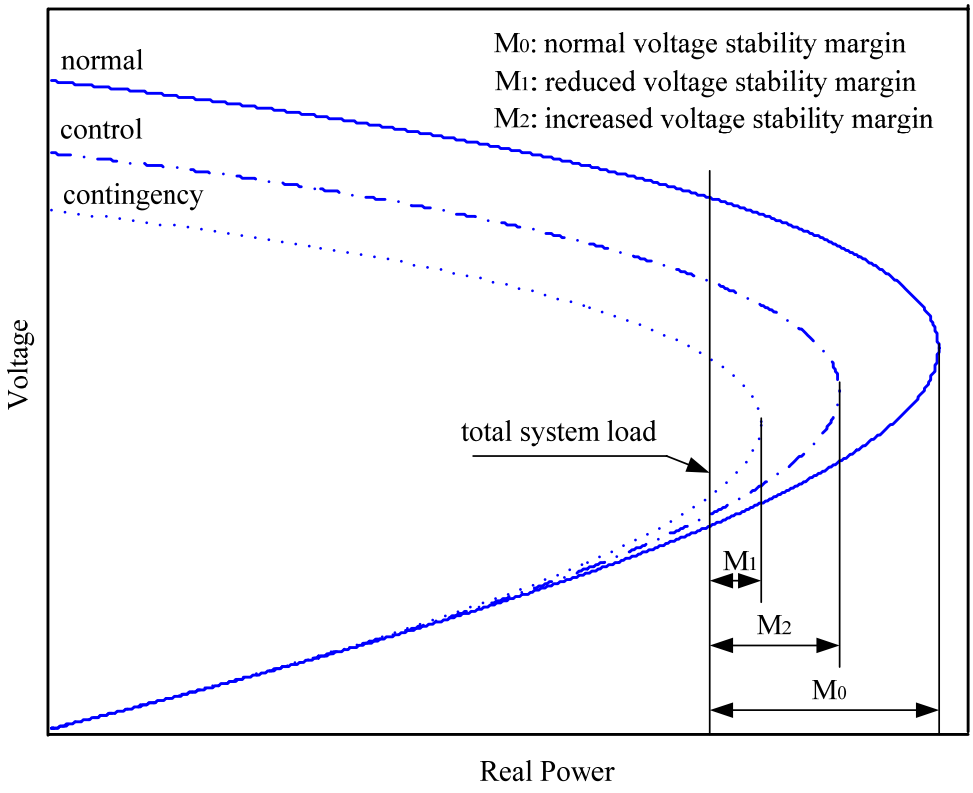

Figure 1.2 Voltage stability margin under different conditions

A power system may have the minimum post-contingency voltage stability margin requirement. For example, the NERC/WECC voltage stability criteria require that:

- The post-contingency voltage stability margin must be greater than 5% for N-1 contingencies;

- The post-contingency voltage stability margin must be greater than 2.5% for N-2 contingencies;
- The post-contingency voltage stability margin must be greater than 0% for N-3 contingencies.

Appropriate power system control devices can be used to increase the voltage stability margin. Figure 1.2 shows the voltage stability margin under different operating conditions and controls.

On the other hand, transient voltage dip is a temporary reduction of the voltage at a point in the electrical system below a threshold [11]. It is also called transient voltage sag. Excessive transient voltage dip may cause fast voltage collapse [4]. In this work, we focus on the transient voltage dip after a fault is cleared. Reference [12] provides information on transient voltage dip criteria following fault clearing related to power system stability. Information was included from utilities, reliability councils, relevant standards, and industry-related papers. The WECC criteria on transient voltage dip are summarized in the following and will be used to illustrate the proposed control planning approach.

The WECC transient voltage dip criteria are specified in a manner consistent with the NERC performance levels of (A) no contingency, (B) an event resulting in the loss of a single element, (C) event(s) resulting in the loss of two or more (multiple) elements, and (D) an extreme event resulting in two or more (multiple) elements removed or cascading out of service conditions, as follows:

- NERC Category A: Not applicable.
- NERC Category B: Not to exceed 25% at load buses or 30% at non-load buses. Not exceed 20% for more than 20 cycles at load buses.

- NERC Category C: Not to exceed 30% at any bus. Not to exceed 20% for more than 40 cycles at load buses.
- NERC Category D: No specific voltage dip criteria.

Figure 1.3 shows the WECC voltage performance parameters with the transient voltage dip criteria clearly illustrated [9]. Again, appropriate power system controls can be utilized to mitigate the post-contingency transient voltage dip problem.

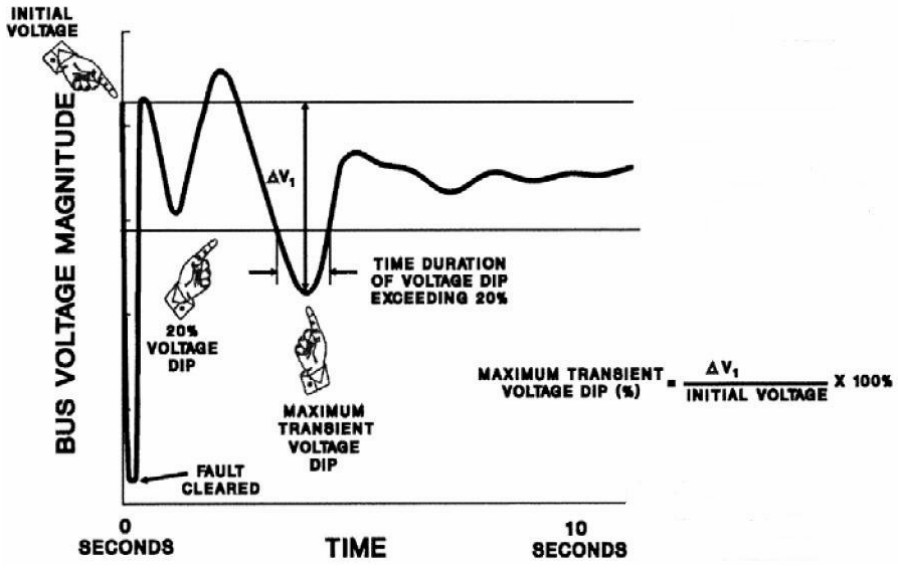

Figure 1.3 Voltage performance parameters for NREC/WECC planning standards

There are two types of control technologies that are today and most certainly will continue to be available to power system control engineers to counteract voltage stability problems. These include:

- Power-electronic based transmission control: static VAR compensators (SVC), thyristor controlled series capacitors (TCSC), Static Compensator (STATCOM) and others that comprise the family of control technology generally referred to as flexible AC transmission systems (FACTS) [13].

- System protection schemes (SPS): mechanically switched shunt/series capacitors (MSC) and others. MSCs have been used for post-contingency control [14, 15, 16, 17, 18, 19, 20, 21].

Of these, the first exerts continuous feedback control action; the second exerts discrete open-loop control action. Based on the response time, SVC and TCSC are often called dynamic VAR resources. MSC belongs to static VAR resources. Both static and dynamic VAR resources belong to reactive (power) control devices. SVC and TCSC are effective countermeasures to increase voltage stability margin and to counteract transient voltage dip problems. However, much cheaper MSC is often sufficient for increasing voltage stability margin [22]. In the MSC family, mechanically switched shunt capacitors are usually cheaper than mechanically switched series capacitors while their effectiveness depends on characteristics of power systems.

On the other hand, SVC and TCSC can effectively mitigate transient voltage dip problems since they can provide almost instantaneous and continuously variable reactive power in response to grid voltage transients. It is hard for MSCs to counteract transient voltage dip problems because they can not be switched on and off rapidly and frequently and because the control amount is discrete. The various functions achievable by different reactive power control devices are summarized in Table 1.1.

Table 1.1 Capabilities of different reactive power control devices

	Static VAR		Dynamic VAR	
	Mechanically switched shunt cap.	Mechanically switched series cap.	SVC	TCSC
Increase voltage stability margin	Yes	Yes	Yes	Yes
Transient voltage dip	No	No	Yes	Yes

A cost comparison of static and dynamic VAR resources is presented in Table 1.2 [23], [24]. The final selection of a specific reactive power control devices should be based on a comprehensive technical and economic analysis.

Table 1.2 Cost comparison for reactive power control devices

	Static VAR		Dynamic VAR	
	Mechanically switched shunt capacitor (500 kV)	Mechanically switched series capacitor (500 kV)	SVC	TCSC
Variable cost ($ million/100 MVar)	0.41	0.75	5.0	5.0
Fixed cost ($ million)	1.3	2.8	1.5	1.5

1.2 Reactive Power Control Planning

The problem addressed in this work is similar to the traditional reactive power planning problem [25], [26], [27], [28]. Generally, the reactive power planning problem can be formulated as a mixed integer nonlinear programming problem to minimize the installation cost of reactive power devices plus the system real power loss or production cost under the normal operating condition subject to a set of power system equality and inequality constraints. In the work described in this dissertation, however, we explicitly target the planning of reactive power controls, i.e., reactive power devices intended to serve as control response for contingency conditions. Thus the system real power loss or production cost is not included in this work.

The reactive power control planning problem can be formulated as follows: minimize the installation cost of reactive power control devices subject to voltage stability margin and/or transient voltage dip requirements under a set of contingencies. It is complex to solve this

problem because of its large solution space, large number of contingencies, difficulty in evaluating the performance of candidate solutions, and lack of efficient mathematical solution technique as described in what follows:

- Large solution space: The space of possible solutions is extremely large, since every bus and every transmission line offer possible control locations. If there are n candidate locations, the number of possible location combinations is 2^n. In addition, the control amount at each candidate location can vary from the minimum allowable value to the maximum allowable value.
- Large number of contingencies: There may exist a large number of N-1, N-2, or even N-3 contingencies having voltage stability problems. In the reactive power control planning, all of these contingencies need to be addressed.
- System performance evaluation: Voltage stability margin and transient voltage dip magnitude and duration are used to measure system performance. However, they can not be analytically expressed as functions of control variables. Measuring these indices under a certain disturbance followed by a specific control action requires numerical simulation.
- Lack of efficient mathematical solution technique: The reactive power control planning to increase voltage stability margin is essentially a MINLP problem. However, there is no general efficient mathematical programming technique for solving MINLP problems.

The existing literature about reactive power control planning can be classified into two groups. The first group deals with static VAR planning to increase voltage stability margin. The second group is about dynamic VAR planning to improve transient voltage performance

or coordinated static and dynamic VAR planning.

There are a few references which address static VAR planning to increase voltage stability margin. Obadina et. al. in [29] developed a method to identify reactive power control that will enhance voltage stability margin. The reactive power control planning problem was formulated in two stages. The first stage involves solving a nonlinear optimization problem which minimizes the control amount at pre-specified locations. The second stage utilizes a mixed integer linear programming which maximizes the number of deleted locations and minimizes the control amount at the remaining locations. Xu, et. al. in [30] used the conventional power flow method to assess the voltage stability margin. The method scale up entire system load in variable steps until the voltage instability point is reached. The modal analysis of the power flow Jacobian matrix was used to determine the most effective reactive power control sites for voltage stability margin improvement. Mansour, et. al. in [31] presented a tool to determine optimal locations for shunt reactive power control devices. The tool first computes the critical modes in the vicinity of the point of voltage collapse. Then system participation factors are used to determine the most suitable sites of shunt reactive power control devices for transmission system reinforcement. Ajjarapu, et. al. in [32] introduced a method of identifying the minimum amount of shunt reactive power support which indirectly maximizes the real power transfer before voltage collapse is encountered. The predictor-corrector optimization scheme was utilized to determine the maximum system loading point. The sensitivity of the voltage stability index derived from the continuation power flow (CPF) was used to select weak buses for locating shunt reactive power devices. A sequential quadratic programming algorithm was adopted to solve the optimization problem with the system security constraint. The objective function is minimizing the total reactive

power injection at the selected weak buses. Overbye, et. al. in [33] presented a method to identify optimal control recommendations to mitigate severe contingencies under which the voltage stability margin is negative (i.e. there is no post-contingency equilibrium). The degree of instability was quantified using the distance in parameter space between the desired operating point and the closest solvable point. The sensitivities of this measure to system controls were used to determine the best way to mitigate the severe contingency. Chen, et. al. in [34] presented a weak bus oriented reactive power planning to counteract voltage collapse. The algorithm identifies weak buses based on the right singular vector of the power flow Jacobian matrix. Then the identified weak buses were selected as candidate shunt reactive power control locations. The smallest singular value was used as the voltage collapse proximity index. The optimization problem was formulated to maximize the minimum singular value. Simulated annealing was applied to search for the final optimal solution. Granville, et. al. in [35] described an application of an optimal power flow [36], solved by a direct interior point method, to restore post-contingency equilibrium. The set of control actions includes rescheduling of generator active power, adjustments on generator terminal voltage, tap changes on LTC transformers, and minimum load shedding. Chang, et. al. in [37] presented a hybrid algorithm based on the simulated annealing method, the Lagrange multiplier, and the fuzzy performance index method for the optimal reactive power control allocation. The proposed procedure has three identified objectives: maximum voltage stability margin, minimum system real power loss, and maximum voltage magnitudes at critical points. Vaahedi, et. al. in [38] evaluated the existing optimal VAR planning/OPF tools for the voltage stability constrained reactive power control planning. A minimum cost reactive power support scheme was designed to satisfy the minimum voltage stability margin requirement given a

pre-specified set of candidate reactive power control locations. The problem formulation does not include the fixed VAR cost. The obtained results indicated that the OPF/VAR planning tools can be used to address the voltage stability constrained reactive power control planning. Additional advantages of these tools are: easier procedures and avoidance of engineering judgment in identifying the reactive power control amount at the candidate locations. Feng, et. al. in [39] identified reactive power controls to increase voltage stability margin under a single contingency using linear programming with the objective of minimizing the control cost. This formulation is suitable to the operational decision making problem. The fixed cost of new controls is not included in the formulation. Yorino, et. al. in [40] proposed a mixed integer nonlinear programming formulation for reactive power control planning which takes into account the expected cost for voltage collapse and corrective controls. The Generalized Benders Decomposition technique was applied to obtain the solution. The convergence of the solution can not be guaranteed because of the nonconvexity of the optimization problem. The proposed model does not include the minimum voltage stability margin requirement.

On the other hand, the available literature on the dynamic VAR planning or coordinated static and dynamic VAR planning is very limited. Donde et. al. [41] presented a method to calculate the minimum capacity requirement of an SVC which satisfies the post-fault transient voltage recovery requirement which is a specific case of the transient voltage dip requirement. Given the target transient voltage recovery time, the minimum SVC capacity was obtained by solving a boundary value problem using numerical shooting methods. The CIGRE report [42] presented a Q-V analysis based procedure for the use by system planners to determine the appropriate mixture of static and dynamic VAR resources at a certain bus. First, the intersection of the required minimum voltage and the post-fault Q-V curve considering the

short-term exponential load characteristic determines the dynamic VAR requirement. Then, the intersection of the required minimum voltage and the post-fault Q-V curve with load modeled as constant power less the dynamic VAR requirement identified in the previous step is the needed amount of static VAR. An approach was presented in [3], [43], and [44] to identify static and dynamic reactive power compensation requirements for an electric power transmission system. First, optimal power flow techniques were used to determine the best locations for reactive power compensation. Then, Q-V analysis with the constant power load model was utilized to find the total amount of reactive compensation at identified locations. Finally, iterative time domain simulations were performed to determine a prudent mix of static and dynamic VAR resources. Kolluri et. al. presented a similar method in [45] to obtain the right mix of static and dynamic VAR resources in a utility company's load pocket. All of the coordinated methods mentioned above use a sequential procedure to allocate static and dynamic VAR resources.

This work develops a systematic approach for coordinated planning of static and dynamic VAR resources to satisfy the requirements of voltage stability margin and/or transient voltage dip under a set of contingencies and thus enhance transmission capability in voltage stability limited systems. We emphasize the coordinated planning of different types of VAR resources to achieve potential economic benefit. The proposed procedures for solving the reactive power control planning problem are based on the following assumptions:

- No new transmission equipment (lines and transformers) is installed, and that generation expansion occurs only at existing generation facilities. This assumption creates conditions that represent the extreme form of current industry trend of relying heavily on control to strengthen and expand transmission capability

without building new transmission or strategically siting new generation.

- Existing continuous controllers: The power system has an existing set of continuous controllers that are represented in the model, including controls on existing generators.
- Candidate controllers: Candidate controllers include mechanically switched shunt/series capacitors or SVCs or coordinated use of any of these in combination.

The proposed reactive power control planning approach requires three basic steps: (i) development of generation/load growth futures, (ii) contingency analysis, (iii) planning of reactive power controls to satisfy the requirements of voltage stability margin and/or transient voltage dip. The overall flowchart of the proposed reactive power control planning algorithm is illustrated in Figure 1.4.

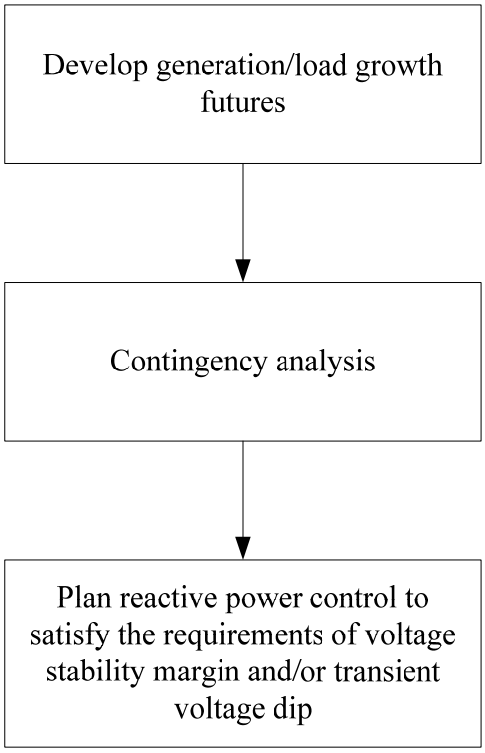

Figure 1.4 Flowchart for reactive power control planning

1.3 Dissertation Organization

The rest of the dissertation is organized as follows:

Chapter 2 presents a methodology to select candidate locations for reactive power controls while satisfying power system performance requirements. Optimal locations of new reactive power controls are obtained by the forward/backward search on a graph representing discrete configuration of controls. Further refinement of the control location and amount is ready to be done using the optimization methods presented in Chapters 3, 4 and 5. The proposed algorithm has complexity linear in the number of feasible reactive power control locations whereas the solution space is exponential.

Chapter 3 proposes a new successive mixed integer programming (MIP) based algorithm to plan the minimum amount of switched shunt and series capacitors to restore equilibria of a power system after severe contingencies. Through parameterization of the severe contingencies, the continuation method is applied to find the critical points. Then, the backward/forward search method and the bifurcation point sensitivities to reactive power controls are used to select candidate locations for switched shunt and series capacitors. Next, a mixed integer programming formulation is proposed to estimate locations and amounts of switched shunt and series capacitors. Finally, mixed integer programming problems with updated information are utilized to further refine the reactive power control locations and amounts.

Chapter 4 presents a successive MIP based method of reactive power control planning to increase voltage stability margin under a set of contingencies. The backward/forward search algorithm and voltage stability margin sensitivities are used to select candidate locations for switched shunt and series capacitors. Optimal locations and amounts of new reactive power

controls are obtained by solving a sequence of mixed integer programming problems.

Chapter 5 proposes a method to coordinate planning of static and dynamic VAR resources when simultaneously considering the performance requirements of voltage stability margin and transient voltage dip. Transient voltage dip sensitivities are derived to select candidate locations for dynamic VAR resources. The successive MIP is proposed to calculate the optimal mix of static and dynamic VAR resources.

Chapter 6 summarizes the specific contribution of the research work and discusses the future work that needs to be done.

CHAPTER 2 LINEAR COMPLEXITY SEARCH ALGORITHM TO LOCATE REACTIVE POWER CONTROL

2.1 Introduction

For reactive power control planning in large scale power systems, the pre-selection of the candidate locations to install new reactive power control devices is important. Usually, candidate control locations are chosen only based on the engineering judgment. There is no guarantee that the selected candidate control locations are effective and sufficient to provide required reactive power support for all concerned contingencies. On the other hand, the computational cost to solve the mixed integer linear/nonlinear programming problem for reactive power control planning may be high if the number of the candidate locations is large.

This chapter presents a method to select appropriate candidate locations for reactive power control devices using the backward/forward search. The proposed method is illustrated in selecting candidate reactive power control locations to increase post-contingency voltage stability margin. The same method will be used to select candidate reactive power control locations to restore post-contingency equilibria and to mitigate transient voltage dip in Chapters 4 and 5 respectively.

The chapter is organized as follows. Some fundamental concepts of voltage stability margin sensitivity are introduced in Section 2.2. Section 2.3 presents the problem formulation. Section 2.4 describes the proposed method of locating reactive power control devices. Numerical results are discussed in Section 2.5. Section 2.6 concludes.

2.2 Voltage Stability Margin Sensitivity

The goal of the chapter is to determine locations for reactive power control devices so as to enable improve voltage stability margin. Here, we formally define the notion of voltage

stability margin sensitivity to parameters, for we use such sensitivities in determining the desired reactive power control locations. The potential for contingencies such as unexpected component (generator, transformer, transmission line) outages in an electric power system often reduces the voltage stability margin to be less than the required value. We are interested in finding effective and economically justified reactive power controls at appropriate locations to steer operating points far away from voltage collapse points by having a pre-specified margin under a set of concerned contingencies.

It is cost-effective to use mechanically switched shunt or series capacitors to increase the voltage stability margin although more expensive dynamic VAR resources such as SVC and TCSC can also be used. The voltage stability margin sensitivity is useful in comparing the effectiveness of the same type of controls at different locations [39]. In this chapter, the margin sensitivity [46], [47], [48], [49], [50] is used in candidate control location selection and contingency screening (see steps 2, 4, and 5 of the overall procedure in Section 2.4.1). In the following, an analytical expression of the margin sensitivity is given, which is what we use for its computation. The details of the margin sensitivity can be found in [46], [47], [49].

Suppose that the steady state of the power system satisfies a set of equations expressed in the vector form

$$F(x, p, \lambda) = 0 \tag{2.1}$$

where x is the vector of state variables, p is any parameter in the power system steady state equations such as the susceptance of shunt capacitors or the reactance of series capacitors, λ is the bifurcation parameter which is a scalar. At the voltage instability point, the value of the bifurcation parameter is equal to λ^*.

A specified system scenario can be parameterized by λ as

$$P_{li} = (1 + K_{lpi}\lambda)P_{li0} \tag{2.2}$$

$$Q_{li} = (1 + K_{lqi}\lambda)Q_{li0} \tag{2.3}$$

$$P_{gj} = (1 + K_{gj}\lambda)P_{gj0} \tag{2.4}$$

Here, P_{li0} and Q_{li0} are the initial loading conditions at the base case where λ is assumed to be zero. K_{lpi} and K_{lqi} are factors characterizing the load increase pattern. P_{gj0} is the real power generation at bus j at the base case. K_{gj} represents the generator load pick-up factor.

The voltage stability margin can be expressed as

$$M = \sum_{i=1}^{n} P_{li}^{*} - \sum_{i=1}^{n} P_{li0} = \lambda^{*} \sum_{i=1}^{n} K_{lpi} P_{li0} \tag{2.5}$$

The sensitivity of the voltage stability margin with respect to the control variable at location i, S_i, is

$$S_i = \frac{\partial M}{\partial p_i} = \frac{\partial \lambda^{*}}{\partial p_i} \sum_{i=1}^{n} K_{lpi} P_{li0} \tag{2.6}$$

If the voltage collapse is due to a saddle-node bifurcation, the bifurcation point sensitivity with respect to the control variable p_i evaluated at the saddle-node bifurcation point is

$$\frac{\partial \lambda^{*}}{\partial p_i} = -\frac{w^{*} F_{p_i}^{*}}{w^{*} F_{\lambda}^{*}} \tag{2.7a}$$

where w is the left eigenvector corresponding to the zero eigenvalue of the system Jacobian F_x, F_λ is the derivative of F with respect to the bifurcation parameter λ and F_{p_i} is the derivative of F with respect to the control variable parameter p_i.

If the voltage collapse is due to a limit-induced bifurcation [51], the bifurcation point sensitivity with respect to the control variable p_i evaluated at the critical limit point (as opposed to at the saddle-node bifurcation point) is

$$\frac{\partial \lambda^*}{\partial p_i} = -\frac{w^*\begin{pmatrix} F^*_{p_i} \\ E^*_{p_i} \end{pmatrix}}{w^*\begin{pmatrix} F^*_{\lambda} \\ E^*_{\lambda} \end{pmatrix}} \tag{2.7b}$$

where $E(x, \lambda, p) = 0$ is the limit equation representing the binding control limit (i.e. Q_i - $Q_i^{\max}$ = 0 representing generator i reaches its reactive power limit), E_λ is the derivative of E with respect to the bifurcation parameter λ, and E_{pi} is the derivative of E with respect to the control variable p_i, w is the nonzero row vector orthogonal to the range of the Jacobian J_c of the equilibrium and limit equations where

$$J_c = \begin{pmatrix} F^*_x \\ E^*_x \end{pmatrix}.$$

2.3 Optimization Problem Formulation

The reactive power control planning problem to increase voltage stability margin can be formulated as follows:

min

$$J = \sum_{i \in \Omega} (C_{fi} + C_{vi} X_i) q_i \tag{2.8}$$

subject to

$$\overline{M}^{(k)}(X_i^{(k)}) \geq M_{\min}, \quad \forall k \tag{2.9}$$

$$X_{i\min} \leq X_i^{(k)} \leq X_i, \quad \forall k \tag{2.10}$$

$$q_i X_{i\min} \leq X_i \leq q_i X_{i\max} \tag{2.11}$$

$$q_i = 0,1 \tag{2.12}$$

The decision variables are X_i, $X_i^{(k)}$ and q_i.

Here,

- C_f is fixed installation cost and C_v is variable cost of reactive power control devices,
- X_i is the size (capacity) of reactive power control devices at location i,
- q_i=1 if the location i is selected for reactive power control expansion, otherwise, q_i=0,
- the superscript k represents the contingency that leads the voltage stability margin to be less than the required value,
- Ω is the set of pre-selected feasible candidate locations to install reactive power control devices,
- $X_i^{(k)}$ is the size of reactive power control devices to be switched on at location i under contingency k,
- M_{min} is an arbitrarily specified voltage stability margin in percentage,
- $\overline{M}^{(k)}(X_i^{(k)})$ is the voltage stability margin under contingency k with control $X_i^{(k)}$, and
- $X_{i\min}$ is the minimum size of reactive power control devices at location i which may be determined by physical and/or environmental considerations.
- $X_{i\max}$ is the maximal size of reactive power control devices at location i which may be determined by physical and/or environmental considerations.

This is a mixed integer nonlinear programming problem, with q being the collection of discrete decision variables and X being the collection of continuous decision variables. For k contingencies that have the voltage stability margin less than the required value and n pre-selected feasible candidate control locations, there are $n(k+2)$ decision variables. In order to reduce the computational cost, it is important to limit the number of candidate control locations to a relative small number for problems of the size associated with practical

large-scale power systems. The candidate control locations could be selected by assessing the relative margin sensitivities [39], [40]. However, there is no guarantee that the pre-selected candidate control locations are appropriate. We propose an algorithm in Section 2.4 for selecting candidate control locations under the assumption that $X_i^{(k)}$ and X_i are fixed at their maximal allowable value, i.e. $X_i^{(k)} = X_i = X_{i\max}$; this reduces the problem to an integer programming problem where the decision variables are locations for reactive power control devices as follows:

min

$$J = \sum_{i\in\Omega}(C_{fi} + C_{vi}X_{i\max})q_i \tag{2.13}$$

subject to

$$\overline{M}^{(k)}(q_i^{(k)}X_{i\max}) \geq M_{\min}, \quad \forall k \tag{2.14}$$

$$q_i^{(k)} \leq q_i, \quad \forall k \tag{2.15}$$

$$q_i^{(k)} = 0,1, \quad \forall k \tag{2.16}$$

$$q_i = 0,1 \tag{2.17}$$

where $q_i^{(k)} = 1$ if the location i is selected for reactive power control expansion under contingency k, otherwise, $q_i^{(k)} = 0$. Here, the decision variables are q_i and $q_i^{(k)}$.

2.4 Methodology

2.4.1 Overall Procedure

In order to select appropriate candidate reactive power control locations the following procedure is applied:

1) Develop generation and load growth future. In this step, the generation/load growth

future is identified, where the future is characterized by a load growth percentage for each load bus and a generation allocation for each generation bus. For example, one future may assume uniformly increasing load at 5% per year and allocation of that load increase to existing generation (with associated increase in unit reactive capability) based on percentage of total installed capacity. Such generation/load growth future can be easily implemented in the continuation power flow (CPF) program [52], [53], [54] by parameterization as shown in (2.2), (2.3) and (2.4).

2) Assess voltage stability by fast contingency screening and the CPF technique. We can use the CPF program to calculate the voltage stability margin of the system under each prescribed contingency. However, the CPF algorithm is time-consuming. If many contingencies must be assessed, the calculation time is large. The margin sensitivity can be used to speed up the procedure of contingency analysis as mentioned in Section 2.2. First, the CPF program is used to calculate (i) the voltage stability margin at the base case, (ii) the margin sensitivity with respect to line admittances, and (iii) the margin sensitivity with respect to bus power injections. The margin sensitivities are calculated according to (2.6). For circuit outages, the resulting voltage stability margin is estimated as

$$M^{(k)} = M^{(0)} + S_l \Delta l \tag{2.18}$$

where $M^{(k)}$ is the voltage stability margin under contingency k, $M^{(0)}$ is the voltage stability margin at the base case, S_l is the margin sensitivity with respect to the admittance of line l, and Δl is the negative of the admittance vector for the outaged circuits.

For generator outages, the resulting voltage stability margin is estimated as

$$M^{(k)} = M^{(0)} + S_g \Delta pq \tag{2.19}$$

where S_g is the margin sensitivity with respect to the power injection of generator g, and Δpq is the negative of the output power of the outaged generators.

Then the contingencies are ranked from most severe to least severe according to the value of the estimated voltage stability margin. After the ordered contingency list is obtained, we evaluate each contingency starting from the most severe one using the accurate CPF program and stop testing after encountering a certain number of sequential contingencies that have the voltage stability margin greater than or equal to the required value, where the number depends on the size of the contingency list. A similar idea has been used in online risk-based security assessment [55].

3) Determination of Expansion Year

Assuming positive load growth but without system enhancement, the voltage stability margin decreases with time as shown in Figure 2.1. The year when the voltage stability margin becomes less than the required value is the time to enhance the transmission system by adding the reactive power control.

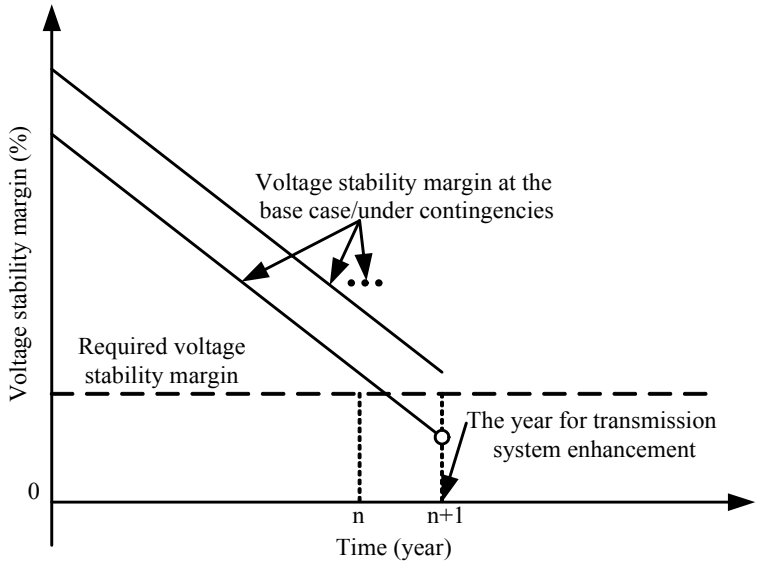

Figure 2.1 Determination of expansion year

4) Choose an initial set of switch locations using the bisection approach for each identified contingency possessing unsatisfactory voltage stability margin according to the following 3 steps:

a) Rank the feasible control locations according to the numerical value of margin sensitivity in descending order with location 1 having the largest margin sensitivity and location *n* having the smallest margin sensitivity.

b) Estimate the voltage stability margin with top half of the switches included as

$$M_{est}^{(k)} = \sum_{i=1}^{\lfloor n/2 \rfloor} X_{i\max}^{(k)} S_i^{(k)} + M^{(k)} \tag{2.20}$$

where $M_{est}^{(k)}$ is the estimated voltage stability margin and $\lfloor n/2 \rfloor$ is the largest integer less than or equal to *n/2*. If the estimated voltage stability margin is greater than the required value, then reduce the number of control locations by one half, otherwise increase the number of control locations by adding the remaining one half.

c) Continue in this manner until we identify the set of control locations that satisfies the voltage stability margin requirement.

5) Refine candidate control locations for each identified contingency possessing unsatisfactory voltage stability margin using the proposed backward/forward search algorithm. We will present the backward/forward search algorithm in Sections 2.4.2 and 2.4.3.

6) Obtain the final candidate control locations as the union of nodes for which voltage stability margin is satisfied, as found in step 5) for every identified contingency.

The current backward/forward search over discrete modes has been done "one contingency at a time". This can be modified by considering all the contingencies simultaneously and it will result in a smaller set of candidate control locations. When we use

the proposed optimization formulation to further refine control locations and compute control amounts, it is expected that the final solution will be less optimal than considering one contingency at each time. In addition, the present approach ensures there is at least one effective candidate location for every contingency having unacceptable margin. The alternative approach does not offer this assurance, and so it could result in one or more contingencies not having an effective control location in the optimization.

The overall procedure for selecting candidate control locations is shown in Figure 2.2.

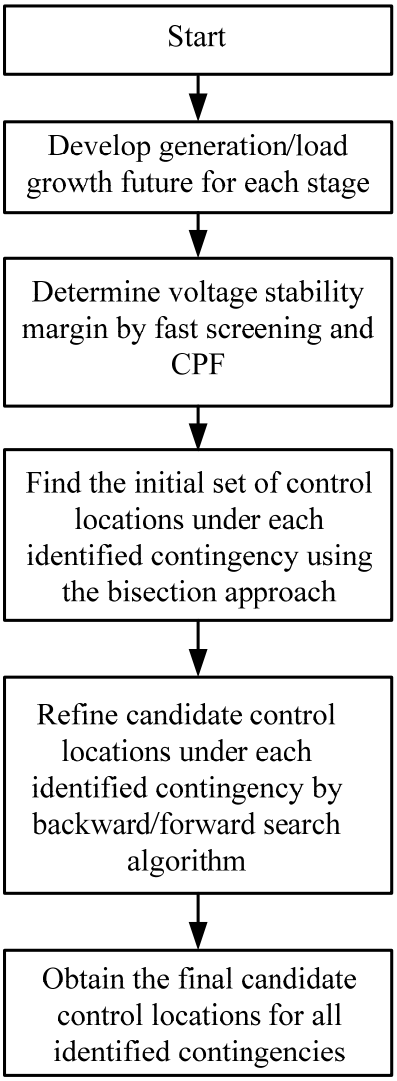

Figure 2.2 Flowchart for candidate control location selection

2.4.2 Backward Search Algorithm

In the proposed search algorithms, we assume that there is only one reactive power switch at each location. The backward/forward search algorithm begins at an initial node representing control configuration and searches from that node in a prescribed direction, either backward or forward. The set of controls corresponding to the selected initial node can be chosen by the bisection approach. The two extreme cases are either searching backward from the node corresponding to all switches included (the strongest node) or forward from the node corresponding to all switches excluded (the weakest node).

Consider the graph where each node represents a configuration of discrete switches, and two nodes are connected if and only if they are different in one switch configuration. The graph has 2^n nodes where n is the number of feasible switches. We pictorially conceive of this graph as consisting of layered groups of nodes, where each successive layer (moving from left to right) has one more switch included (or "closed") than the layer before it, and the t^{th} layer (where $t=0,\ldots,n$) consists of a number of nodes equal to $n!/t!(n-t)!$. Figure 2.3 illustrates the graph for the case of 4 switches.

The backward search algorithm has 4 steps.

1) Select the node corresponding to all switches in the initial set that are closed.

2) For the selected node, check if voltage stability margin requirement is satisfied for the concerned contingency on the list. If not, then stop, the solution corresponds to the previous node (if there is a previous node, otherwise use the forward search algorithm).

3) For the selected node, exclude (open) the switch that has the smallest margin sensitivity. We denote this as switch i^*:

$$i^* = \arg\left\{\min_{i\in\Omega_c} S_i^{(k)}\right\} \tag{2.21}$$

where $\Omega_c = \{\text{set of closed switches for the selected node}\}$, $S_i^{(k)}$ is the margin sensitivity with respect to the susceptance of shunt capacitors or the reactance of series capacitors under contingency k, at location i.

4) Choose the neighboring node corresponding to the switch i^* being off. If there is more than one switch identified in step 3, i.e. $|i^*|>1$, then choose any one of the switches in i^* to exclude (open). Return to step 2.

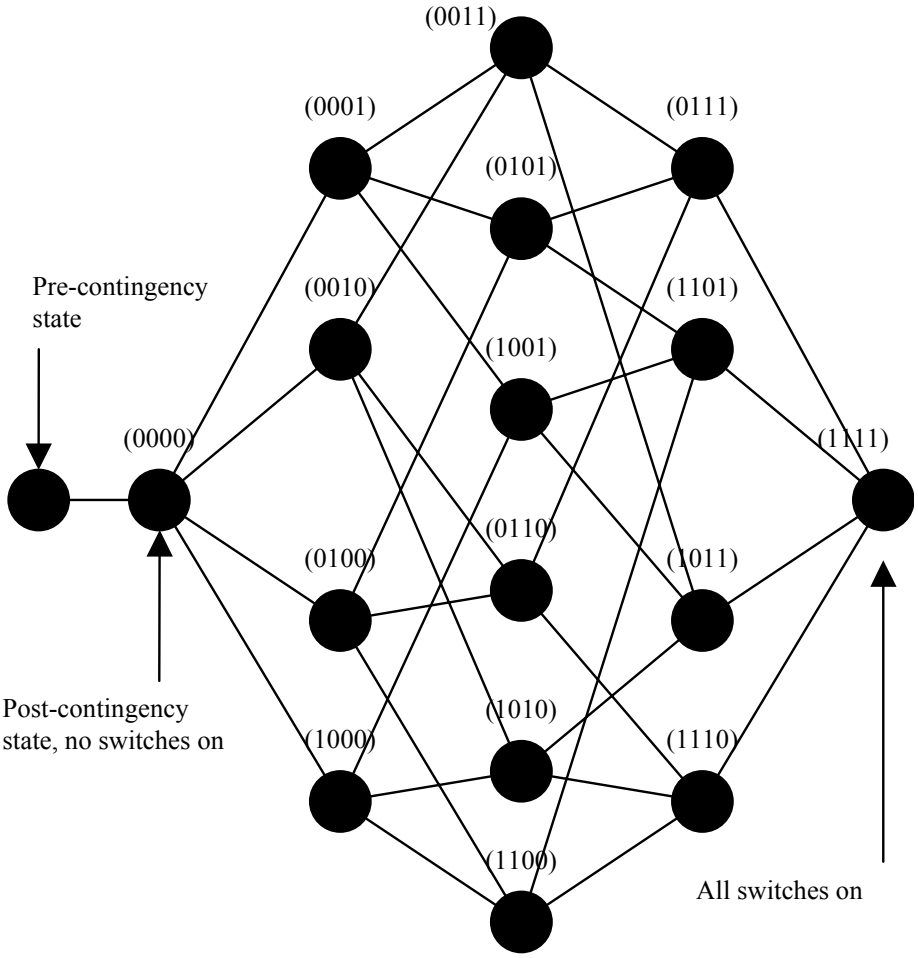

Figure 2.3 Graph for 4-switch problem

2.4.3 Forward Search Algorithm

The forward search algorithm has 4 steps.

1) Start from an initial node.
2) For the selected node, check if voltage stability margin requirement is satisfied for the concerned contingency on the list. If yes, then stop, the solution corresponds to the previous node (if there is a previous node, otherwise use the backward search algorithm).
3) For the selected node, include (close) the switch that has the largest margin sensitivity. We denote this as switch j^*:

$$j^* = \arg\{\max_{j\in\Omega} S_j^{(k)}\} \tag{2.22}$$

where Ω = {set of pre-selected feasible locations}.

4) Choose the neighboring node corresponding to the switch j^* being closed. If there is more than one switch identified in step 3, i.e. $|j^*|>1$, then choose any one of the switches in j^* to include (close). Return to step 2.

2.5 Case Study

The proposed method has been applied to a test system adapted from [56] as shown in Figure 2.4 to identify good candidate locations for shunt or series reactive power control devices. Table 2.1 shows the system loading and generation of the base case.

In the simulations, the following conditions are implemented unless stated otherwise:

- Constant power loads;
- Required voltage stability margin is assumed to be 15%;
- In computing voltage stability margin, the power factor of the load bus remains

constant when the load increases, and load and generation increase are proportional to their base case value.

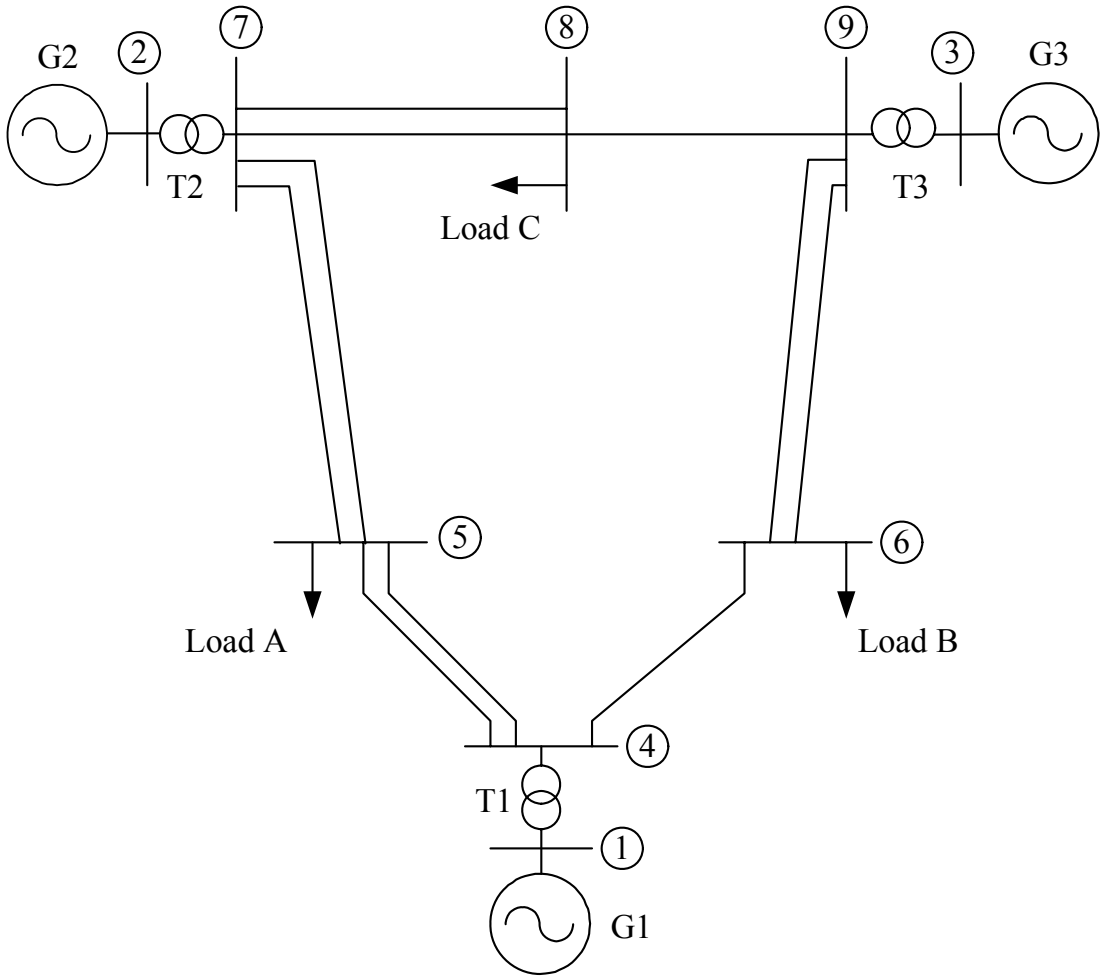

Figure 2.4 Modified WECC nine-bus system

Table 2.1 Base case loading and dispatch for the modified WECC system

	Load A	Load B	Load C	G1	G2	G3
MW	147.7	106.3	118.2	128.9	163.0	85.0
MVar	59.1	35.5	41.4	41.4	16.7	-1.9

A contingency analysis was performed on the system. For each bus, consider the simultaneous outage of 2 components (generators, lines, transformers) connected to the bus. There exist 2 contingencies that reduce the post-contingency voltage stability margin to be less than 15%, and they are shown in Table 2.2.

Table 2.2 Voltage stability margin under contingencies for the WECC system

Contingency	Voltage stability margin (%)
1. Outage of lines 5-4A and 5-4B	4.73
2. Outage of transformer T1 and line 4-6	4.67

2.5.1 Candidate Location Selection for Shunt Capacitors

We first select candidate locations for shunt capacitors under the outage of lines 5-4A and 5-4B. Table 2.3 summarizes the steps taken by the backward search algorithm in terms of switch sensitivities, where we have assumed the susceptance of shunt capacitors to be installed at feasible buses $X_i^{(k)} = X_i = X_{i\max} = 0.3\ p.u.$ We take the initial network configuration as six shunt capacitors at buses 4, 5, 6, 7, 8, and 9 are switched on. The voltage stability margin with all six shunt capacitors switched on is 17.60% which is greater than the required value of 15%. Therefore, the number of switches can be decreased to reduce the cost. At the first step of the backward search, we compute the margin sensitivity for all six controls as listed in the 4th column. From this column, we see that the row corresponding to the shunt capacitor at bus 4 has the minimal sensitivity. So in this step of backward search, this capacitor is excluded from the list of control locations indicated by the strikethrough. Continuing in this manner, in the next three steps of the backward search we exclude shunt capacitors at buses 6, 9, and 8 sequentially. However, as seen from the last column of Table

2.3, with only 2 controls at buses 5 and 7, the voltage stability margin is unacceptable at 13.98%. Therefore the final solution must also include the capacitor excluded in the last step, i.e., the shunt capacitor at bus 8. The location of these controls are intuitively pleasing given that, under the contingency, Load A, the largest load, must be fed radially by a long transmission line, a typical voltage stability problem.

Table 2.3 Steps taken in the backward search algorithm for shunt capacitor planning

No.		no cntrl.	6 cntrls.	5 cntrls. (reject #6)	4 cntrls. (reject#5)	3 cntrls. (reject#4)	2 cntrls. (reject#3)
1	Sens. of shunt cap. at bus 5	0.738	0.879	0.877	0.874	0.868	0.851
2	Sens. of shunt cap. at bus 7	0.334	0.384	0.384	0.382	0.379	0.370
3	Sens. of shunt cap. at bus 8	0.240	0.284	0.284	0.282	~~0.278~~	
4	Sens. of shunt cap. at bus 9	0.089	0.106	0.105	~~0.104~~		
5	Sens. of shunt cap. at bus 6	0.046	0.056	~~0.056~~			
6	Sens. of shunt cap. at bus 4	0.019	~~0.023~~				
	Loadability (MW)	389.8	437.7	437.0	435.4	432.4	424.3
	Voltage stability margin (%)	4.73	17.60	17.42	16.99	16.17	13.98

Figure 2.5 shows the corresponding search via the graph. In the figure, node O represents the origin configuration of discrete switches from where the backward search originates, and node R represents the restore configuration associated with a minimal set of discrete switches which satisfies the voltage stability margin requirement (this is the node where the search ends).

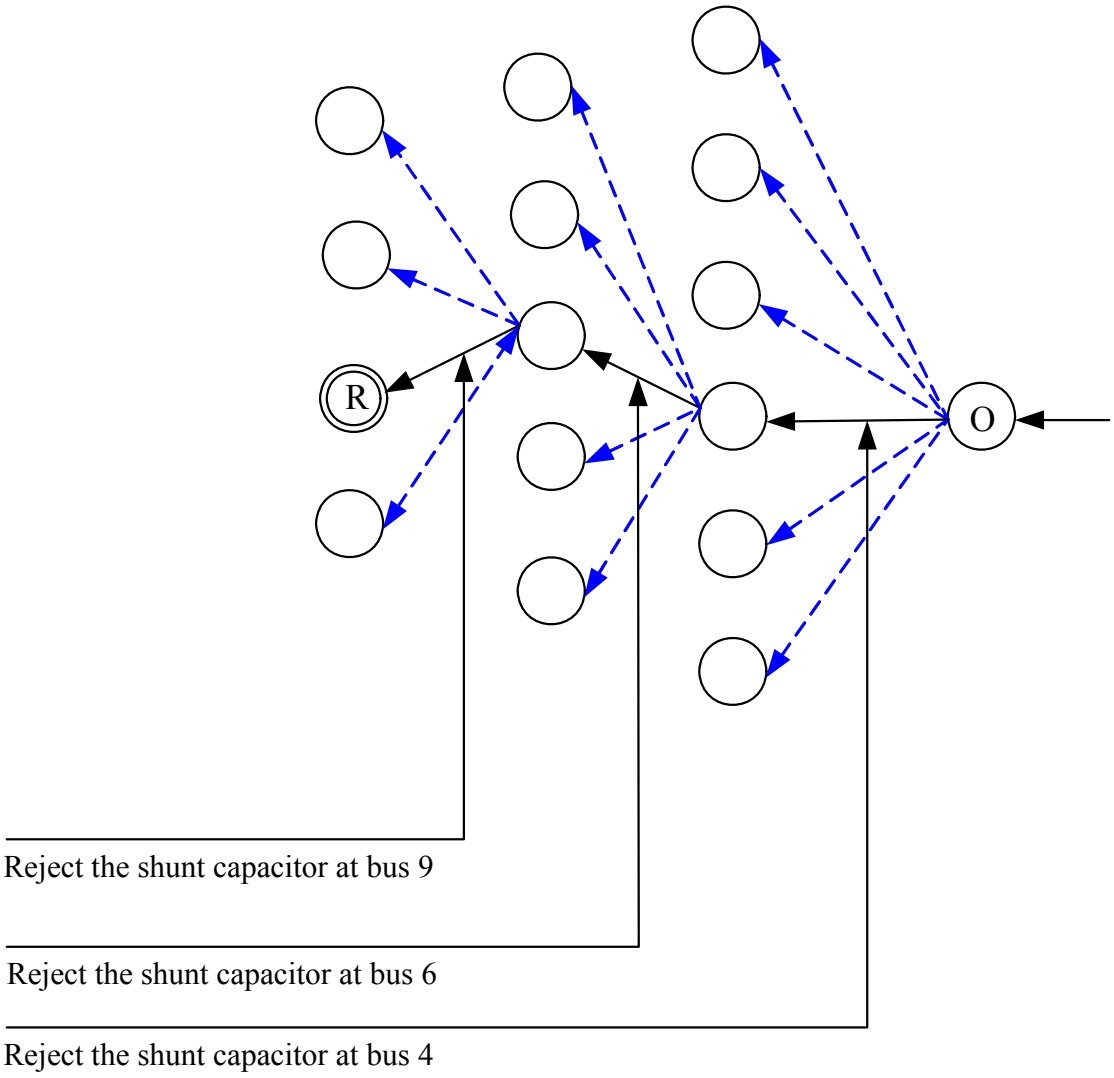

Figure 2.5 Graph for the backward search algorithm for shunt capacitor planning

Table 2.4 summarizes the steps taken by the forward search algorithm in terms of switch sensitivities, where we have again assumed $X_i^{(k)} = X_i = X_{i\max} = 0.3\ p.u.$ The initial network configuration is chosen as no shunt capacitor is switched on. Here, at each step, the switch with the maximal margin sensitivity is included (closed), as indicated in each column by the numerical value within the box. Figure 2.6 shows the corresponding search via the graph.

Table 2.4 Steps taken in forward search algorithm for shunt capacitor planning

No.		no cntrl	1 cntrl add # 1	2 cntrls add # 2	3 cntrls add # 3
1	Sensitivity of shunt cap. at bus 5	0.738			
2	Sensitivity of shunt cap. at bus 7	0.334	0.356		
3	Sensitivity of shunt cap. at bus 8	0.240	0.256	0.265	
4	Sensitivity of shunt cap. at bus 9	0.089	0.095	0.098	
5	Sensitivity of shunt cap. at bus 6	0.046	0.049	0.050	
6	Sensitivity of shunt cap. at bus 4	0.019	0.021	0.021	
	Loadability (MW)	389.8	413.3	424.2	432.4
	Voltage stability margin (%)	4.73	11.04	13.97	16.17

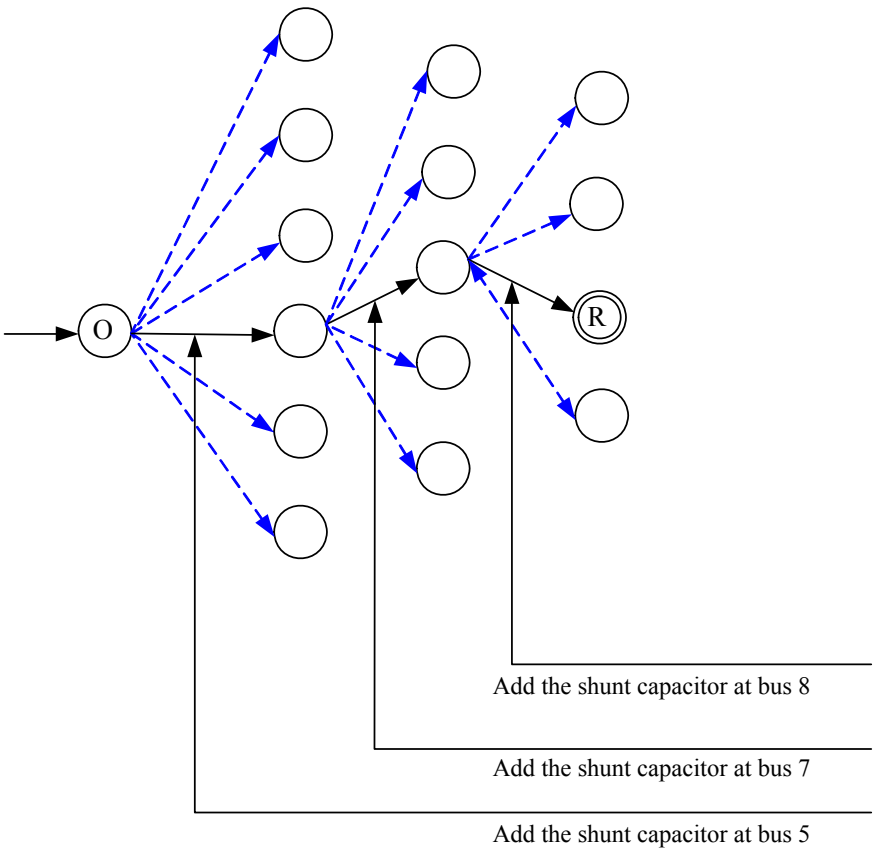

Figure 2.6 Graph for the forward search algorithm for shunt capacitor planning

The solution obtained from the forward search algorithm is the same as that obtained using the backward search algorithm: shunt capacitors at buses 5, 7 and 8. This is guaranteed to occur if switch sensitivities do not change as the switching configuration is changed, i.e., if the system is linear. We know power systems are nonlinear, and the changing sensitivities across the columns for any given row of Tables 2.3 or 2.4 confirm this. However, we also observe from Tables 2.3 and 2.4 that the sensitivities do not change much, thus giving rise to the agreement between the algorithms. For large systems, however, we do not expect the two algorithms to identify the same solution. And of course, neither algorithm is guaranteed to identify the optimal solution. But both algorithms will generate good solutions. This will facilitate good reactive power planning design.

The optimization problem of (2.13)-(2.17) could be solved by a traditional integer programming method, e.g., the branch-and-bound algorithm. However, our algorithm has complexity linear in the number of switches n, whereas branch and bound has worst case complexity of order 2^n. The improvement in complexity comes at the expense of optimality: branch-and-bound finds an optimal solution, whereas our algorithm finds a solution that is set-wise minimal. There can exist more than one minimal set solution, and to compute an optimal solution, one will have to examine all of them which we avoid for the sake of complexity gain.

For the outage of transformer T1 and line 4-6, the solution obtained by the forward search algorithm is: shunt capacitors at buses 4 and 5. Therefore, the final candidate locations for shunt capacitors are buses 4, 5, 7, and 8 which guarantee that the voltage stability margin under all prescribed N-2 contingencies is greater than the required value.

2.5.2 Candidate Location Selection for Series Capacitors

Series capacitor compensation has two effects that are not of concern for shunt capacitor compensation. First, series capacitors can expose generator units to risk of sub-synchronous resonance (SSR), and such risk must be investigated. Second, series capacitors also have significant effect on real power flows. In our work, we intend that both shunt and series capacitors be used as contingency-actuated controls (and therefore temporary) rather than continuously operating compensators. As a result, the significance of how they affect real power flows may decrease. However, the SSR risk is still a significant concern. To address this issue, the planner must identify *a-priori* lines where series compensation would create SSR risk and eliminate those lines from the list of candidates.

Table 2.5 summarizes the steps taken by the forward search algorithm to plan series capacitors for the outage of lines 5-4A and 5-4B, where we have assumed the reactance of series capacitor to be installed in feasible lines $X_i^{(k)} = X_i = X_{i\max} = 0.06\ p.u.$ We take the initial network configuration as no series capacitor is switched on. At each step, the switch with the maximal margin sensitivity is included, as indicated in each column by the numerical value within the box. Figure 2.7 shows the corresponding search via the graph.

Table 2.5 shows that the solution utilizes 2 controls. These controls are series capacitors in lines 5-7A and 5-7B. Again, the location of these controls are intuitively pleasing.

For the outage of transformer T1 and line 4-6, the solution obtained by the forward algorithm is the same as the result for the outage of lines 5-4A and 5-4B: series capacitors in lines 5-7A and 5-7B. Therefore, the final candidate locations for series capacitors are lines 5-7A and 5-7B.

Table 2.5 Steps taken in forward search algorithm for series capacitor planning

No.		no cntrl	1 cntrl add # 1	2 cntrls add # 2
1	Sensitivity of series cap. in line 5-7A	4.861		
2	Sensitivity of series cap. in line 5-7B	4.861	4.575	
3	Sensitivity of series cap. in line 8-9	1.747	2.056	
4	Sensitivity of series cap. in line 4-6	0.288	0.332	
5	Sensitivity of series cap. in line 7-8A	0.046	0.045	
6	Sensitivity of series cap. in line 7-8B	0.046	0.045	
7	Sensitivity of series cap. in line 6-9A	0.008	0.007	
8	Sensitivity of series cap. in line 6-9B	0.008	0.007	
	Loadability (MW)	389.8	415.3	439.8
	Voltage stability margin (%)	4.73	11.58	18.16

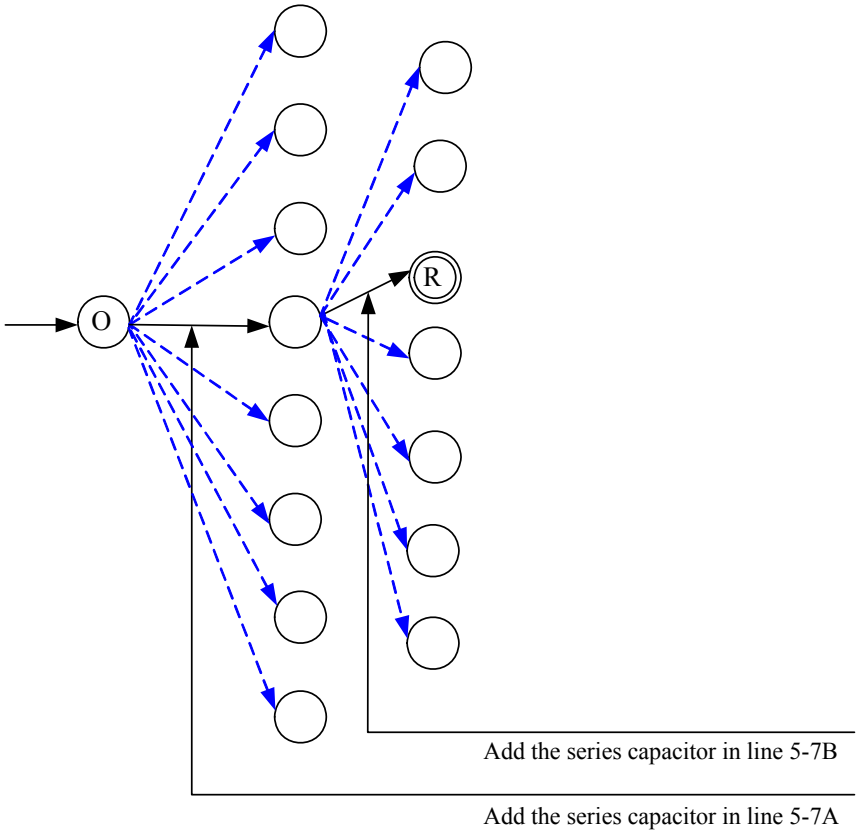

Figure 2.7 Graph for the forward search algorithm for series capacitor planning

2.6 Summary

This chapter presents a method of locating reactive power controls in electric transmission systems to satisfy performance requirements under contingencies. Further refinement of control locations and amounts is ready to be done using the optimization methods proposed in Chapters 3, 4 and 5. The proposed algorithm has complexity linear in the number of feasible reactive power control locations whereas the solution space is exponential. The effectiveness of the method is illustrated by using a modified WSCC 9-bus system. The results show that the method works satisfactorily to find good candidate locations for reactive power controls.

CHAPTER 3 REACTIVE POWER CONTROL PLANNING TO RESTORE EQUILIBRIUM

3.1 Introduction

Voltage instability is one of the major threats to power system operation [24]. Severe contingencies such as tripping of heavily loaded transmission lines or outage of large generating units can cause voltage instability when no new equilibrium of the power system exists (i.e. the voltage stability margin is negative) after contingencies. In face of the loss of equilibrium voltage instability, switched shunt and series capacitors are generally effective control candidates [10], [18], [24]. The problem, also referred to as power flow solvability restoration, was initially addressed through the so-called non-divergent power flow [33], [57]. An approach for determining the minimum load shedding to restore an equilibrium of a power system based on the total equilibrium tracing method [58] was proposed in [59]. In [40], a mixed integer nonlinear programming formulation was presented for the reactive power control planning problem. Load shedding was used to guarantee the existence of power flow solution after contingencies.

In this chapter, we present a new approach for planning the minimum amount of switched shunt and series capacitors to restore the voltage stability when no equilibria exist due to severe contingencies. Through parameterization of severe contingencies, the continuation method is applied to find the critical point. Then, the backward/forward search algorithm with linear complexity is used to select candidate locations for switched shunt and series capacitors. Next, a mixed integer programming formulation is proposed for estimating locations and amounts of switched shunt and series capacitors to withstand a planned set of contingencies. A sequence of MIP problems with updated information is utilized to further

refine the control locations and amounts. Because our problem formulation is linear, it is scalable and at the same time provides good solutions as evidenced by the application to the New England 39-bus system.

3.2 Contingency Analysis via Parameterization and Continuation

A power system may lose equilibrium after severe contingencies. The techniques of contingency parameterization and continuation can be used for planning corrective reactive power controls to restore equilibrium. This section presents the technique of contingency analysis via parameterization and continuation. There are basically two types of contingencies that cause voltage instability. One is branch type of contingency such as the outage of transformers or transmission lines. The other is node type of contingency such as the outage of generators or shunt reactive power compensation devices. The contingency parameterization for both types of contingencies is as follows.

3.2.1 Parameterization of Branch Outage

The set of parameterized power flow equations at bus *i* for the outage of branch *br* connecting bus *i* to bus *m* is as follows:

$$\begin{cases} P_i^{inj} - V_i \sum_{j\in L(i), j\neq m} V_j (G_{ij}\cos\theta_{ij} + B_{ij}\sin\theta_{ij}) - V_i V_m (G_{im}^{new}\cos\theta_{im} + B_{im}^{new}\sin\theta_{im}) \\ -V_i^2 G_{ii}^{new} - P_{im}(V_i, V_m, \lambda) = 0 \\ Q_i^{inj} - V_i \sum_{j\in L(i), j\neq m} V_j (G_{ij}\sin\theta_{ij} - B_{ij}\cos\theta_{ij}) - V_i V_m (G_{im}^{new}\sin\theta_{im} - B_{im}^{new}\cos\theta_{im}) + V_i^2 B_{ii}^{new} \\ -Q_{im}(V_i, V_m, \lambda) = 0 \end{cases} \tag{3.1}$$

where $L(i) = \{j : Y_{ij} \neq 0,\ j \neq i\}$ is the set of buses that are directly connected to bus *i* through transmission lines, $G_{ij}+jB_{ij}$ is the (i, j) element of the bus admittance matrix, $G_{ii}+jB_{ii}$ is the i*th* diagonal element of the bus admittance matrix, θ_{ij} is the voltage angle difference between bus

i and bus *j*, V_i and V_j are voltage magnitude of bus *i* and bus *j* respectively, $G_{ii}^{new} + jB_{ii}^{new}$ is the new *k*th diagonal element of the bus admittance matrix and $G_{im}^{new} + jB_{im}^{new}$ is the new (*i*, *m*) element of the bus admittance matrix after branch *br* has been removed from the system, P_i^{inj} and Q_i^{inj} are real power and reactive power injections at bus *i*. $P_{im}(V_i, V_m, \lambda)$ and $Q_{im}(V_i, V_m, \lambda)$ are defined as follows:

$$P_{im}(V_i, V_m, \lambda) = (1-\lambda)\{V_i V_m (G_{im}^{br} \cos\theta_{im} + B_{im}^{br} \sin\theta_{im}) + V_i^2 G_{ii}^{br}\} \tag{3.2}$$

$$Q_{im}(V_i, V_m, \lambda) = (1-\lambda)\{V_i V_m (G_{im}^{br} \sin\theta_{im} - B_{im}^{br} \cos\theta_{im}) - V_i^2 B_{ii}^{br}\} \tag{3.3}$$

When λ=0, (3.1) represents the original set of power flow equations before contingency. On the other hand, when λ=1, (3.1) is the new set of power flow equations with branch *br* removed. Figure 3.1 shows the parameterization of branch outage where Y_c is one-half of the total shunt admittance per phase to neutral of the branch and Y_{series} is the total series admittance per phase of the branch. Similar formulation was presented in [60] which uses the parameterization of branch outage to investigate the effects of varying branch parameters on power flow solutions.

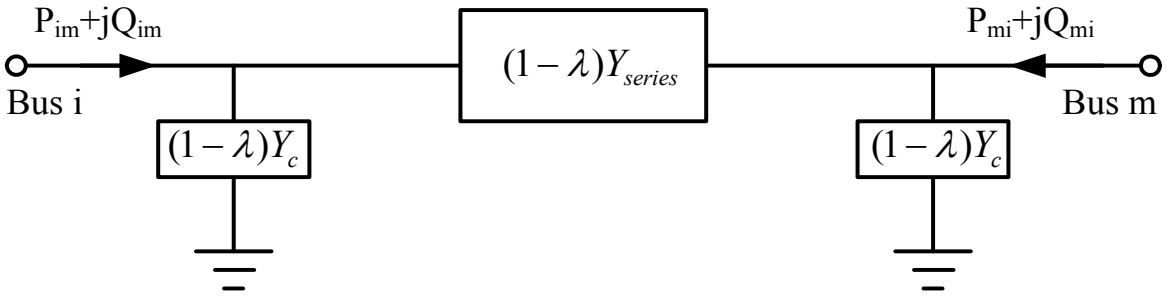

Figure 3.1 Parameterization of branch outage

3.2.2 Parameterization of HVDC Link Outage

A high voltage direct current (HVDC) link consists of a rectifier and an inverter as shown in Figure 3.2. The rectifier side of the HVDC link may be represented as a load consuming positive real and reactive power. On the other hand, the inverter side of the HVDC link may be represented as a generator providing positive real power and negative reactive power (i.e. absorbing positive reactive power) [61].

The set of parameterized power flow equations at the terminal bus *r* of the rectifier side of the HVDC link is as follows:

$$\begin{cases} -P_{rec}(1-\lambda) - V_r \sum_{j \in L(r)} V_j (G_{rj} \cos\theta_{rj} + B_{rj} \sin\theta_{rj}) - V_r^2 G_{rr} = 0 \\ -Q_{rec}(1-\lambda) - V_r \sum_{j \in L(r)} V_r (G_{rj} \sin\theta_{rj} - B_{rj} \cos\theta_{rj}) + V_r^2 B_{rr} = 0 \end{cases} \tag{3.4}$$

where P_{rec}, Q_{rec} are real and reactive power as seen from the AC network at the rectifier terminal bus under the normal operating condition respectively.

The set of parameterized power flow equations at the terminal bus *i* of the inverter side of the HVDC link is as follows:

$$\begin{cases} P_{inv}(1-\lambda) - V_i \sum_{j \in L(i)} V_j (G_{ij} \cos\theta_{ij} + B_{ij} \sin\theta_{ij}) - V_i^2 G_{ii} = 0 \\ -Q_{inv}(1-\lambda) - V_i \sum_{j \in L(i)} V_j (G_{ij} \sin\theta_{ij} - B_{ij} \cos\theta_{ij}) + V_i^2 B_{ii} = 0 \end{cases} \tag{3.5}$$

where P_{inv}, Q_{inv} are real and reactive power as seen from the AC network at the inverter terminal bus under the normal operating condition respectively.

When λ=0, (3.4) and (3.5) represent the set of power flow equations before contingency. On the other hand, when λ=1, (3.4) and (3.5) are the set of power flow equations after the HVDC link is shut down.

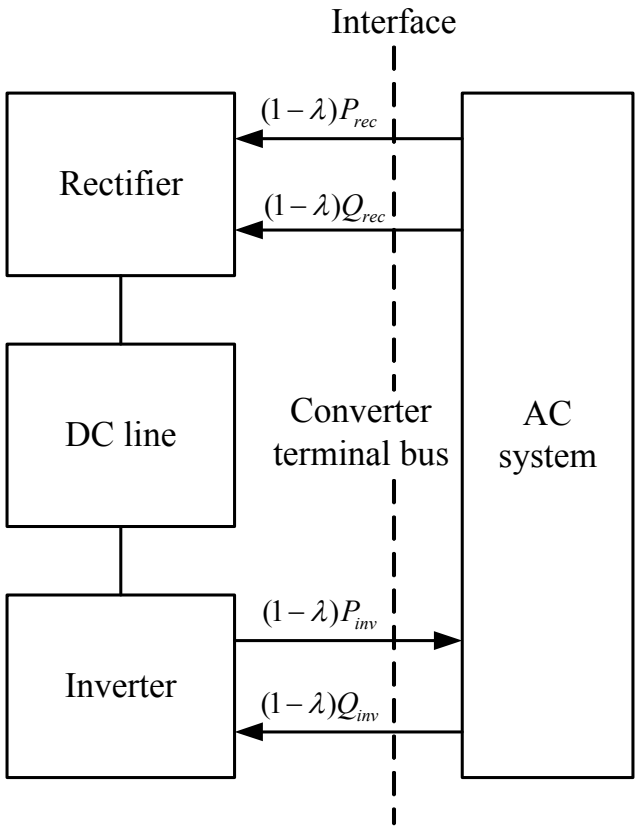

Figure 3.2 Parameterization of HVDC link outage

3.2.3 Parameterization of Generator Outage

The parameterized power flow equation at bus *i* for the outage of the generator at that bus is as follows:

$$\begin{cases} P_{gi}(1-\lambda) - P_{di} - V_i \sum_{j \in L(i)} V_j (G_{ij} \cos\theta_{ij} + B_{ij} \sin\theta_{ij}) - V_i^2 G_{ii} = 0 \\ Q_{gi}(1-\lambda) - Q_{di} - V_i \sum_{j \in L(i)} V_j (G_{ij} \sin\theta_{ij} - B_{ij} \cos\theta_{ij}) + V_i^2 B_{ii} = 0 \end{cases} \quad (3.6)$$

where P_{gi} and P_{di} are generator real power output and load real power respectively, Q_{gi} and Q_{di} are generator reactive power output and load reactive power respectively. For a generator of PV type, Q_{gi} is the reactive power output under the normal operating condition.

Assume the real power generation loss P_{gi} is reallocated among the available generators as

follows:

$$\sum_{z \neq i} \Delta P_{gz} = P_{gi} \tag{3.7}$$

Where ΔP_{gz} is the specified real power increase of available generator z after the faulted generator i is removed from the system.

The parameterized power flow equation at generator bus z for the outage of the generator at bus i is as follows:

$$P_{gz} + \lambda \Delta P_{gz} - P_{dz} - V_z \sum_{j \in L(i)} V_j (G_{zj} \cos\theta_{zj} + B_{zj} \sin\theta_{zj}) - V_z^2 G_{zz} = 0 \tag{3.8}$$

When λ=0, (3.6) and (3.8) represent the power flow equations before contingency. On the other hand, when λ=1, (3.6) and (3.8) are the power flow equations after the generator at bus i is shut down.

3.2.4 Continuation Method

Generally, the parameterized set of equations representing steady state operation of a power system under a *N-k* contingency (where $k \geq 1$) can be represented as

$$F(x, p, \lambda) = 0 \tag{3.9}$$

where x is the vector of state variables, p is any controllable parameter such as the susceptance of switched shunt capacitors or the reactance of switched series capacitors, λ is the scalar uncontrollable bifurcation parameter which parameterizes the simultaneous outage of k components. Specifically, when λ=0, the set of parameterized steady state equations represents the one before contingency. On the other hand, when λ=0, the set of parameterized steady state equations is the one after all faulted k components are removed from the system.

The continuation method can be used to find the critical point associated with a contingency precisely and reliably. In addition, the sensitivity information obtained as a

by-product of the continuation method is useful for reactive power control planning. Generally, the continuation method can be applied to solve the following problem [62].

Given a mapping F: $R^n \times R \times R \to R^n$, find solutions to $F(x, p, \lambda) = 0$ where $x \in R^n, p \in R, \lambda \in R$.

Power system engineers have applied the continuation method to continuation power flow on varying bus power injections [52], [53], [54] and on varying branch parameters [60]. [63] combines the continuation power flow on varying bus injections and branch parameters to study the existence of power flow solution under severe contingencies. During the continuation process, λ is increased from 0 to 1 as shown in Figure 3.3. If there is a stable operating point after a contingency, the continuation method can find this point with $\lambda^* = 1$. If there is no power flow solution following a contingency, the continuation method will obtain a critical point with $\lambda^* < 1$.

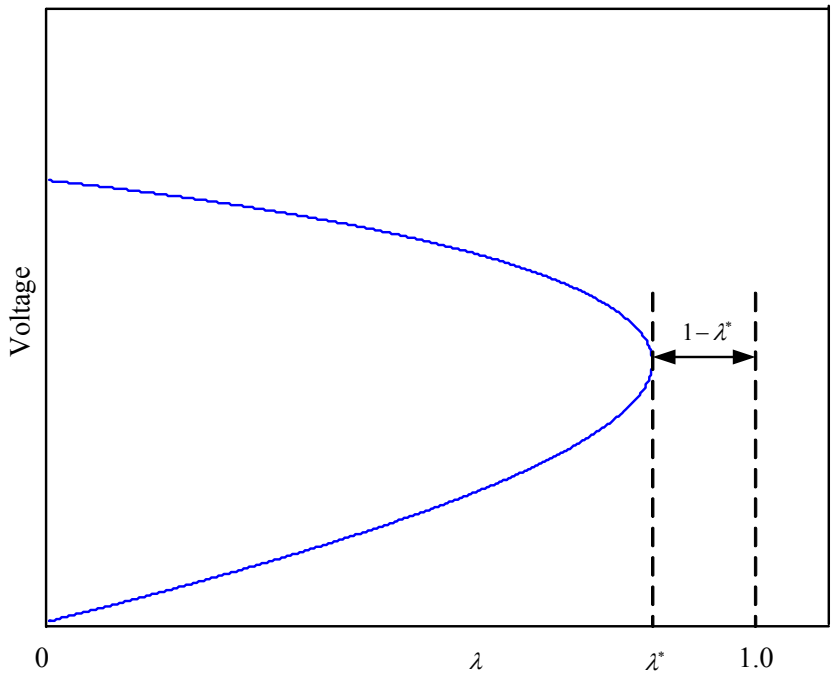

Figure 3.3 Bifurcation curve obtained by the continuation method

If the critical point is due to saddle-node bifurcation, the sensitivity of the critical point with respect to the control variable p is

$$\frac{\partial \lambda^*}{\partial p} = -\frac{w^* F_p^*}{w^* F_\lambda^*} \tag{3.10}$$

where F_λ^* is the derivative of F with respect to the bifurcation parameter λ evaluated at the critical point and F_p^* is the derivative of F with respect to the control variable p evaluated at the critical point. In the following section, the bifurcation parameter sensitivity is used to plan cost-effective reactive power controls against voltage collapse.

If the critical point is due to a limit-induced bifurcation, the sensitivity of the critical point to the control variable p_i is

$$\frac{\partial \lambda^*}{\partial p_i} = -\frac{w^* \begin{pmatrix} F_{p_i}^* \\ E_{p_i}^* \end{pmatrix}}{w^* \begin{pmatrix} F_\lambda^* \\ E_\lambda^* \end{pmatrix}} \tag{3.11}$$

where $E(x, \lambda, p) = 0$ is the limit equation representing the binding control limit, E_λ is the derivative of E with respect to the bifurcation parameter λ, and E_{pi} is the derivative of E with respect to the control variable p_i, w is the nonzero row vector orthogonal to the range of the Jacobian J_c of the equilibrium and limit equations where

$$J_c = \begin{pmatrix} F_x^* \\ E_x^* \end{pmatrix} \tag{3.12}$$

3.3 Formulation for Reactive Power Control Planning

3.3.1 Flowchart for Reactive Power Control Planning

A flowchart for planning minimum switched shunt and series capacitors to restore an equilibrium of a power system after severe contingencies is shown in Figure 3.4.

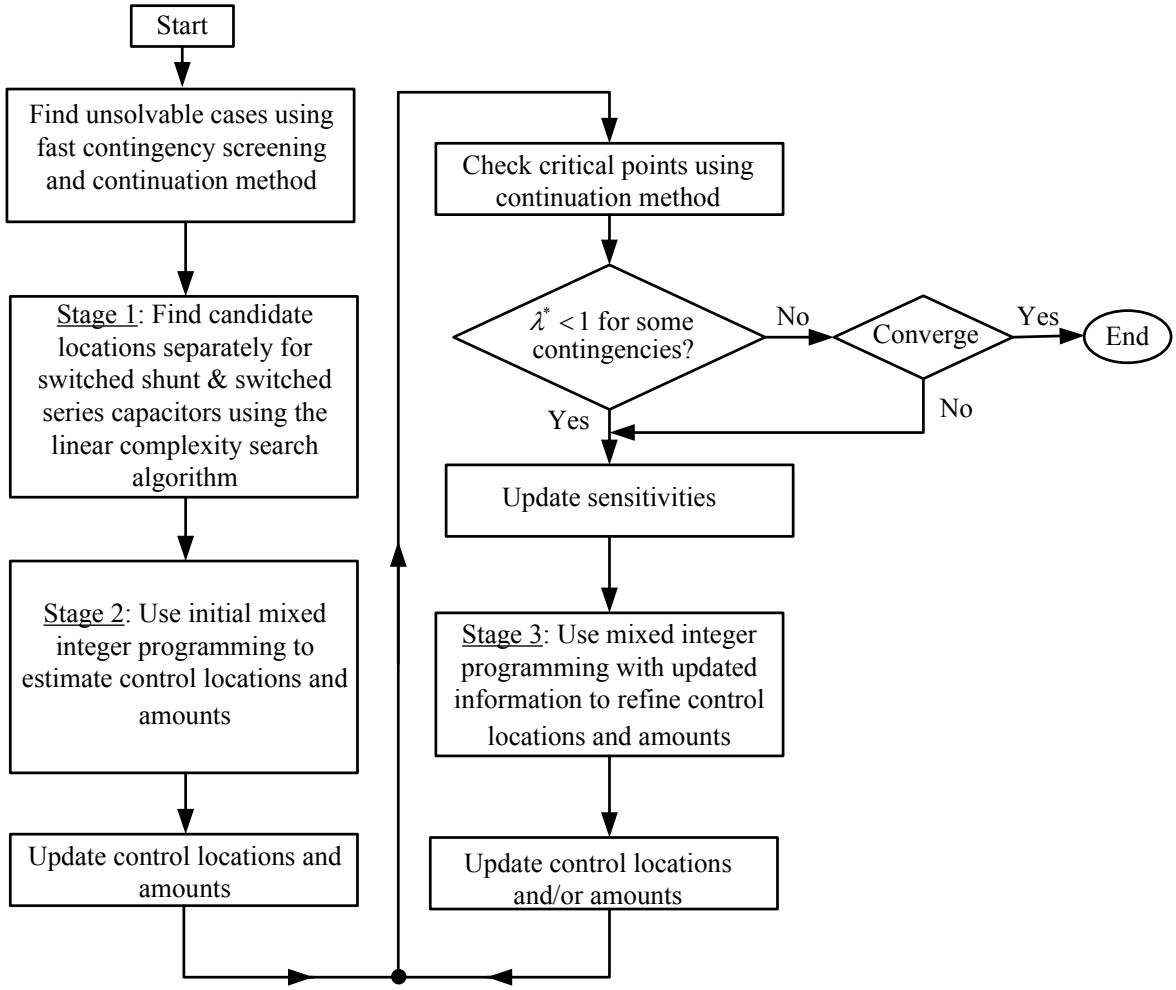

Figure 3.4 Flowchart for the minimum reactive power control planning to restore equilibrium

3.3.2 Voltage Stability Analysis

The procedure of voltage stability analysis is similar to the one presented in Section 2.4.1, Chapter 2. The contingencies are ranked from most severe to least severe according to the value of the estimated voltage stability margin using the procedure introduced in Section 2.4.1. After the ordered contingency list is obtained, we evaluate each contingency starting from the most severe one using the accurate continuation method and stop testing after encountering a certain number of sequential contingencies having the critical value λ^* greater than or equal to

one, where the number depends on the size of the contingency list.

3.3.3 Selection of Candidate Control Locations

An important step in the reactive power control planning problem is the selection of the candidate locations for switched shunt and series capacitors. The backward/forward search algorithm with linear complexity proposed in Chapter 2 can be used to find candidate locations separately for switched shunt and switched series capacitors under every contingency where we use the contingency parameterization instead of the conventional generation/load parameterization. It is assumed that the capacities of switched shunt and switched series capacitors are fixed at the maximum allowable value in this step.

3.3.4 Formulation of Initial Mixed Integer Programming

In the previous step, we find the candidate locations for switched shunt and series capacitors separately. There exists redundancy of control locations when we plan switched shunt and series capacitors together. We use a mixed integer programming (MIP) to estimate control locations and amounts. The MIP minimizes control installation cost while restoring equilibria (i.e. the bifurcation parameter at the critical point λ^* is greater than or equal to one):

minimize

$$J = \sum_{i \in \Omega_1} (C_{vi} B_i + C_{fi} q_i) + \sum_{j \in \Omega_2} (C_{vj} X_j + C_{fj} q_j) \tag{3.13}$$

subject to

$$\left(\sum_{i \in \Omega_1} S_i^{(k)} B_i^{(k)} + \sum_{j \in \Omega_2} S_j^{(k)} X_j^{(k)} \right) + \lambda^{*(k)} \geq 1, \quad \forall k \tag{3.14}$$

$$B_{i\min} \leq B_i^{(k)} \leq B_i, \quad \forall k \tag{3.15}$$

$$X_{j\min} \leq X_j^{(k)} \leq X_j, \quad \forall k \tag{3.16}$$

$$B_{i\min} q_i \le B_i \le B_{i\max} q_i \tag{3.17}$$

$$X_{j\min} q_j \le X_j \le X_{j\max} q_j \tag{3.18}$$

$$q_i, q_j = 0,1 \tag{3.19}$$

The decision variables are $B_i^{(k)}$, B_i, q_i, $X_j^{(k)}$, X_j, and q_j.

Here,

- C_f is fixed installation cost and C_v is variable cost of switched shunt or series capacitors,
- B_i is the size (susceptance) of the switched shunt capacitor at location i,
- X_j is the size (reactance) of the switched series capacitor at location j,
- q_i=1 if location i is selected for reactive power control expansion, otherwise, q_i=0 (the same to q_j),
- the superscript k represents the contingency under which there is no equilibrium,
- Ω_1 is the set of candidate locations to install switched shunt capacitors,
- Ω_2 is the set of candidate locations to install switched series capacitors,
- $B_i^{(k)}$ is the size of the shunt capacitor to be switched on at location i under contingency k,
- $X_j^{(k)}$ is the size of the series capacitor to be switched on at location j under contingency k,
- $S_i^{(k)}$ is the sensitivity of the bifurcation parameter with respect to the susceptance of the shunt capacitor at location i under contingency k,
- $S_j^{(k)}$ is the sensitivity of the bifurcation parameter with respect to the reactance of the series capacitor at location j under contingency k,

- $\lambda^{*(k)}$ is the bifurcation parameter evaluated at the critical point under contingency k and without controls,
- $B_{i\min}$ is the minimum size of the switched shunt capacitor at location i,
- $B_{i\max}$ is the maximum size of the switched shunt capacitor at location i,
- $X_{j\min}$ is the minimum size of the switched series capacitor at location j, and
- $X_{j\max}$ is the maximum size of the switched series capacitor at location j.

Note that constraints (3.17) and (3.18) guarantee that (i) if the size of the switched shunt or series capacitors is zero, the location variable is zero, (ii) if the size of the switched shunt or series capacitors is nonzero, the location variable is nonzero, (iii) if the location variable is zero, the size of the switched shunt or series capacitors is zero, and (iv) if the location variable is non-zero, the size of the switched shunt or series capacitors is nonzero. Therefore the objective function in (3.13) is equivalent to

$$J' = \sum_{i\in\Omega_1}(C_{vi}B_i + C_{fi})q_i + \sum_{j\in\Omega_2}(C_{vj}X_j + C_{fj})q_j \tag{3.20}$$

However, the objective function in (3.13) is preferred because it is a mixed integer linear objective function instead of the mixed integer nonlinear objective function in (3.20).

For k contingencies that do not have post-fault equilibria and n pre-selected candidate control locations, there are $n(k+2)$ decision variables and $k+3n+2kn$ constraints. The number of candidate control locations can be limited to a relative small number even for problems of the size associated with practical power systems by using the backward/forward search algorithm. Therefore, computational cost for solving the above MIP is not high even for large power systems.

The output of the MIP is the control locations and amounts for all k contingencies and the

combined control location and amount. For each concerned contingency, the identified controls are switched on, and λ^* is recalculated to check if an equilibrium is restored. However, because we use the linear sensitivity to estimate the effect of the variations of control variables on the value of the bifurcation parameter at the critical point, there may be contingencies that have λ^* less than one after the network configuration is updated according to the results of the MIP. Also, the obtained solution may not be optimal after one iteration of MIP. The control locations and/or amounts can be further refined by solving a second-stage mixed integer programming with updated information. In the successive MIP, we use updated sensitivity at each iteration.

3.3.5 Formulation of MIP with Updated Information

The successive MIP is formulated to minimize the total control installation cost subject to the constraint of equilibrium restoration, as follows:

minimize

$$J = \sum_{i\in\Omega_1}(C_{vi}\overline{B}_i + C_{fi}\overline{q}_i) + \sum_{j\in\Omega_2}(C_{vj}\overline{X}_j + C_{fj}\overline{q}_j) \tag{3.21}$$

subject to

$$\left(\sum_{i\in\Omega_1}\overline{S}_i^{(k)}(\overline{B}_i^{(k)} - B_i^{(k)}) + \sum_{j\in\Omega_2}\overline{S}_j^{(k)}(\overline{X}_j^{(k)} - X_j^{(k)})\right) + \overline{\lambda}^{*(k)} \geq 1 \;\forall k \tag{3.22}$$

$$B_{i\min} \leq \overline{B}_i^{(k)} \leq \overline{B}_i, \quad \forall k \tag{3.23}$$

$$X_{j\min} \leq \overline{X}_j^{(k)} \leq \overline{X}_j, \quad \forall k \tag{3.24}$$

$$B_{i\min}\overline{q}_i \leq \overline{B}_i \leq B_{i\max}\overline{q}_i \tag{3.25}$$

$$X_{j\min}\overline{q}_j \leq \overline{X}_j \leq X_{j\max}\overline{q}_j \tag{3.26}$$

$$\overline{q}_i, \overline{q}_j = 0,1 \tag{3.27}$$

The decision variables are $\overline{B}_i^{(k)}$, $\overline{B}_i$, $\overline{q}_i$, $\overline{X}_j^{(k)}$, $\overline{X}_j$ and $\overline{q}_j$.

Here,

- $\overline{B}_i$ is the new size of the switched shunt capacitor at location *i*,
- $\overline{X}_j$ is the new size of the switched series capacitor at location *j*,
- $\overline{q}_i$ and $\overline{q}_j$ are new binary control location variables,
- $\overline{S}_i^{(k)}$ is the updated sensitivity of the bifurcation parameter with respect to the susceptance of the switched shunt capacitor at location *i* under contingency *k*,
- $\overline{S}_j^{(k)}$ is the updated sensitivity of the bifurcation parameter with respect to the reactance of the switched series capacitor at location *j* under contingency *k*,
- $\overline{B}_i^{(k)}$ is the new size of the switched shunt capacitor at location *i* under contingency k,
- $\overline{X}_j^{(k)}$ is the new size of the switched series capacitor at location *j* under contingency k, and
- $\overline{\lambda}^{*(k)}$ is the updated bifurcation parameter evaluated at the critical point under contingency k.

The above successive MIP will end until all post-contingency equilibria are restored and there is no significant movement of the decision variables from the previous MIP solution as shown in Figure 3.4.

3.4 Application to New England System

The proposed method has been applied to the New England 39 bus system [64] shown in Figure 3.5.

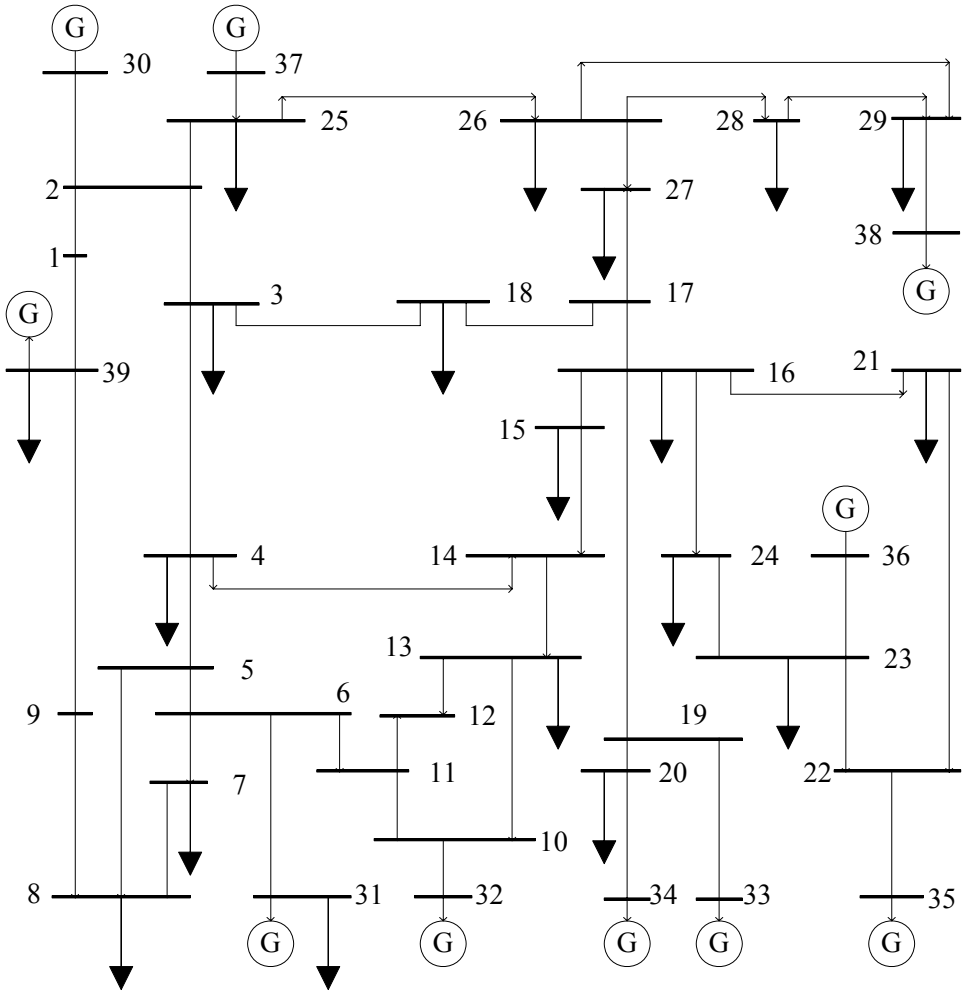

Figure 3.5 New England 39-bus test system

In the simulations, the following conditions are implemented unless stated otherwise:

- Constant power load model is used;
- For generator outage, the generation loss is picked up by available generators proportional to their base case value;
- The branch-and-bound method and the primal-dual interior-point method are used

to solve the mixed integer programming problems [66].

- The parameter values adopted in the optimization problem are given in Table 3.1.

Table 3.1 Parameter values in the optimization formulation to restore equilibrium

	Shunt capacitor	Series capacitor
Maximum size (p.u.)	2.0	50% compensation
Minimum size (p.u.)	$B_{imin}=10^{-3}$	$X_{jmin}=10^{-3}$

Considering all N-1 contingencies, the voltage stability of the system is analyzed by the fast contingency screening and the continuation method presented in section 3.3.2. There exist 2 contingencies that cause the system to be unsolvable as shown in Table 3.2.

Table 3.2 Critical point under two severe contingencies for the New England system

Contingency	λ^*
(1). Outage of the generator at bus 38	0.92
(2). Outage of the generator at bus 39	0.82

The candidate control locations are determined based on the backward/forward search algorithm presented in Section 2.4. The best five candidate buses to install switched shunt capacitors are buses 1, 9, 28, 29, 39. The best three candidate lines to install switched series capacitors are lines 1-2, 6-7, 25-26. For these candidate locations, the reactive power control planning algorithm presented in Section 3.3 was carried out.

The optimal control allocations are shown in Table 3.3 indicating that a switched series capacitor of 0.0205 p.u. on line 1-2, a switched series capacitor of 0.0150 p.u. on line 25-26 and a switched shunt capacitor of 0.5094 p.u. at bus 39. The total cost for the control allocation is $7.1355 million. If only switched shunt capacitors were chosen as candidate

reactive power controls, the total cost for the control allocation is $9.3569 million which is 31.1% higher than that of coordinated planning of switched shunt and series capacitors. This result shows that benefit could be obtained by coordinated planning of different types of discrete reactive power controls. Table 3.4 gives the verified results of the reactive power control planning with the continuation method. Clearly, the value of the bifurcation parameter at the critical point λ^* under the concerned contingencies is increased to the required value of 1.0 p.u. with the planned controls. The iteration number in the second column represents the number of times of performing the MIP to obtain the optimal solution.

Table 3.3 Control allocations for shunt and series capacitors to restore equilibrium

Candidate locations for shunt and series capacitors	Maximal size limit (p.u.)	Overall optimal control allocation (p.u.)	Solution to cont. (1) (p.u.)	Solution to cont. (2) (p.u.)
Bus 39	2.0	0.5094	0	0.5094
Line 1-2	0.0205	0.0205	0.0205	0.0205
Line 25-26	0.0162	0.0150	0.0150	0

Table 3.4 Critical point under planned controls

Candidate control	Iteration number for MIP	λ^* for cont. (1)	λ^* for cont. (2)
Shunt and series capacitors	3	1.00	1.00

The computation in the proposed reactive control planning method is done only to (a) calculate the critical points and sensitivities and (b) solve the optimization. It is only in calculating the critical points and sensitivities that we must deal with the full size of the power system. Computation associated with optimization is mainly affected by the number of candidate controls.

3.5 Summary

This chapter presents an optimization based method of planning reactive power controls in electric transmission systems to restore equilibria under severe contingencies. The planned reactive power controls are capable to serve a planned set of contingencies. Optimal locations and amounts of new switch controls are obtained by solving a sequence of mixed integer programming problems. The proposed approach can handle a large-scale power system because it significantly reduces the computational cost by fully utilizing the information of the sensitivity of the bifurcation parameter at the critical point. The effectiveness of the method is illustrated by applying to the New England 39 bus system. The results show that the method works satisfactorily to plan switched shunt and series capacitors to restore post-contingency equilibria. After the equilibria are restored, the post-contingency voltage stability margin of the system can be increased to a required value by solving an optimization problem proposed in the next chapter.

CHAPTER 4 REACTIVE POWER CONTROL PLANNING TO INCREASE VOLTAGE STABILITY MARGIN

4.1 Introduction

In the last chapter, we propose an algorithm to restore equilibria of a power system under severe contingencies by adding the minimum amount of switched shunt/series capacitors. After the equilibrium is restored under each severe contingency, the voltage stability margin is just equal to zero. At this point, a small disturbance can result in a negative voltage stability margin and cause voltage collapse. On the other hand, the potential for moderate contingencies often leads to small voltage stability margins. We need to add more reactive power control devices to increase the voltage stability margin to be greater than a pre-specified value.

In this chapter, a method is presented for the reactive power control planning to increase post-contingency voltage stability margin. Mechanically switched shunt and series capacitors are used as the reactive power control means. Instead of considering only the most severe contingency or considering several contingencies sequentially [65] the proposed planning method considers multiple contingencies simultaneously. The backward/forward search algorithm with linear complexity is used to select candidate control locations. An initial mixed integer linear programming (MILP) formulation using voltage stability margin sensitivities is proposed to estimate reactive power control locations and amounts from the candidates. The objective function of the MILP is to minimize the total installation cost including fixed cost and variable cost of new controls while satisfying the voltage stability margin requirement under contingencies. A sequence of MILP with updated margin sensitivities is proposed to refine control amounts and/or locations from the initial MILP result until the voltage stability

margin requirement is satisfied and there is no significant movement of the decision variables from the previous MIP solution. The CPF program is utilized to check the true voltage stability margin after each MILP. This iterative process is required to account for system nonlinearities. The branch-and-bound and primal-dual interior-point methods [66] are used to solve the optimization problem. Because the optimization formulation is linear, it is fast, yet it provides good solutions for large-scale power systems compared with nonlinear optimization formulations.

The following assumptions are made in this chapter:

- The system planner has identified a-priori lines where series compensation would create sub-synchronous resonance (SSR) risk and has eliminated those lines from the list of candidates.
- Voltage magnitude control is addressed as a refinement following identification of the reactive power resources necessary to satisfy the voltage stability margin requirements.

The chapter is organized as follows. Section 4.2 describes the proposed method of the reactive power control planning. Numerical results are discussed in Section 4.3. Section 4.4 concludes.

4.2 Algorithm of Reactive Power Control Planning

The proposed reactive power control planning approach requires three stages: (1) select candidate control locations, (2) use MIP to estimate control locations and amounts from stage 1 locations, and (3) use MIP with updated information to refine control amounts and/or locations from stage 2 locations and amounts. The overall procedure for the reactive power

control planning is shown in Figure 4.1 which integrates the above mentioned steps.

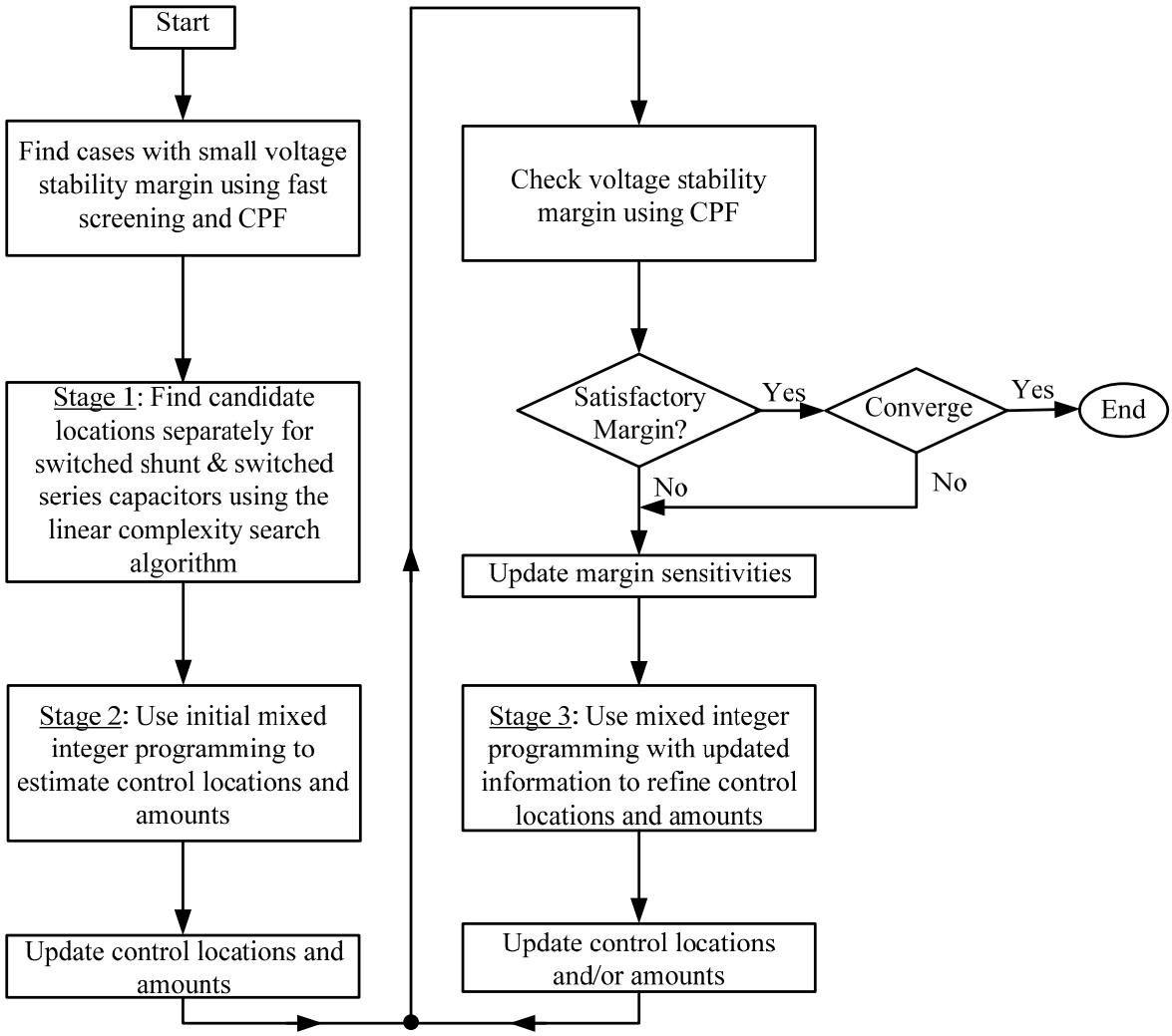

Figure 4.1 Flowchart for the reactive power control planning to increase voltage stability margin

4.2.1 Selection of Candidate Control Locations

The backward/forward search algorithm with linear complexity presented in Chapter 2 is used to find candidate locations separately for switched shunt and switched series capacitors

under every contingency.

4.2.2 Formulation of Initial Mixed Integer Programming

In stage 1, we find the candidate locations for switched shunt and series capacitors separately. In this stage, we use a mixed integer programming (MIP) to estimate control locations and amounts from candidate control locations. The MIP minimizes the total control installation cost while increasing the voltage stability margin to a required percentage x for each concerned contingency.

minimize

$$J = \sum_{i \in \Omega_1} (C_{vi} B_i + C_{fi} q_i) + \sum_{j \in \Omega_2} (C_{vj} X_j + C_{fj} q_j) \tag{4.1}$$

subject to

$$\sum_{i \in \Omega_1} S_i^{(k)} B_i^{(k)} + \sum_{j \in \Omega_2} S_j^{(k)} X_j^{(k)} + M^{(k)} \geq x P_{l0}, \quad \forall k \tag{4.2}$$

$$B_{i\min} \leq B_i^{(k)} \leq B_i, \quad \forall k \tag{4.3}$$

$$X_{j\min} \leq X_j^{(k)} \leq X_j, \quad \forall k \tag{4.4}$$

$$B_{i\min} q_i \leq B_i \leq B_{i\max} q_i \tag{4.5}$$

$$X_{j\min} q_j \leq X_j \leq X_{j\max} q_j \tag{4.6}$$

$$q_i, q_j = 0,1 \tag{4.7}$$

The decision variables are $B_i^{(k)}$, B_i, q_i, $X_j^{(k)}$, X_j, and q_j.

Here,

- C_{fi} is fixed installation cost and C_{vi} is variable cost of mechanically switched shunt capacitors,
- C_{fj} is fixed installation cost and C_{vj} is variable cost of mechanically switched series

capacitors,

- B_i is the size (susceptance) of the switched shunt capacitor at location i,
- X_j is the size (reactance) of the switched series capacitor at location j,
- q_i=1 if location i is selected for reactive power control expansion, otherwise, q_i=0 (the same to q_j),
- the superscript k represents the contingency under which there is insufficient voltage stability margin,
- Ω_1 is the set of candidate locations to install switched shunt capacitors,
- Ω_2 is the set of candidate locations to install switched series capacitors,
- $B_i^{(k)}$ is the size of the shunt capacitor to be switched on at location i under contingency k,
- $X_j^{(k)}$ is the size of the series capacitor to be switched on at location j under contingency k,
- $S_i^{(k)}$ is the sensitivity of the voltage stability margin with respect to the susceptance of the shunt capacitor at location i under contingency k,
- $S_j^{(k)}$ is the sensitivity of the voltage stability margin with respect to the reactance of the series capacitor at location j under contingency k,
- x is an arbitrarily specified voltage stability margin in percentage,
- P_{l0} is the forecasted system load,
- $M^{(k)}$ is the voltage stability margin under contingency k and without controls,
- $B_{i\min}$ is the minimum size of the switched shunt capacitor at location i,
- $B_{i\max}$ is the maximum size of the switched shunt capacitor at location i,

- $X_{j\min}$ is the minimum size of the switched series capacitor at location j, and
- $X_{j\max}$ is the maximum size of the switched series capacitor at location j.

Note that, we identify the minimum set of switched shunt and series capacitors to restore equilibrium points under severe contingencies using the successive MIP in Chapter 3. We may then increase the voltage stability margin for these contingencies to the required value along with other contingencies having insufficient voltage stability margin. In order to minimize the total installation cost of switched shunt and series capacitors, the previously identified switched shunt and series capacitors can be utilized to increase the voltage stability margin for other contingencies. For example, if B_i amount of switched shunt capacitor is identified at location i and $B_i^{(k)}$ amount ($B_i^{(k)}$ can be zero under other contingencies) of switched shunt capacitor at location i needs to be switched on under contingency k to restore the equilibrium point, there will be no cost for using B_i-$B_i^{(k)}$ and no fixed cost for using $B_{i\max}$-B_i to increase the voltage stability margin. Consequently, the fixed as well as variable cost for B_i-$B_i^{(k)}$ is set to be zero and the fixed cost for $B_{i\max}$-B_i is set to be zero in the above MIP problem.

For k contingencies that have the voltage stability margin less than the required value and n selected candidate control locations, there are $n(k+2)$ decision variables and $k+3n+2kn$ constraints. For the same reason as in Section 3.3.4, the computational cost for solving the above mixed integer programming formulation is not high even for large-scale power systems. The branch-and-bound and primal-dual interior-point methods are used to solve this mixed integer programming problem.

The output of the mixed integer programming problem is the control locations and amounts for all k contingencies and the combined control location and amount. Then the network configuration is updated by switching in the controls under each contingency. After

that, the voltage stability margin is recalculated using CPF to check if sufficient margin is achieved for each concerned contingency. This step is necessary because the voltage stability margin nonlinearly depends on control variables, and our mixed integer programming algorithm uses linear margin sensitivities to estimate the effect of variations of control variables on the voltage stability margin. As a result, there may be contingencies that have insufficient voltage stability margin after updating the network configuration according to results of the initial mixed integer programming problem. Also, the obtained solution may not be optimal after one iteration of MIP. The control locations and/or amounts are further refined by recomputing margin sensitivities (with updated network configuration) under each concerned contingency, and solving a second-stage successive MIP with updated information, as described in the next subsection.

4.2.3 Formulation of MIP with Updated Information

The successive MIP is formulated to minimize the total control installation cost subject to the constraint of the voltage stability margin requirement, as follows:

minimize

$$J = \sum_{i\in\Omega_1}(C_{vi}\overline{B}_i + C_{fi}\overline{q}_i) + \sum_{j\in\Omega_2}(C_{vj}\overline{X}_j + C_{fj}\overline{q}_j) \tag{4.8}$$

subject to

$$\left(\sum_{i\in\Omega_1}\overline{S}_i^{(k)}(\overline{B}_i^{(k)} - B_i^{(k)}) + \sum_{j\in\Omega_2}\overline{S}_j^{(k)}(\overline{X}_j^{(k)} - X_j^{(k)})\right) + \overline{M}^{(k)} \geq xP_{l0}, \quad \forall k \tag{4.9}$$

$$B_{i\min} \leq \overline{B}_i^{(k)} \leq \overline{B}_i, \quad \forall k \tag{4.10}$$

$$X_{j\min} \leq \overline{X}_j^{(k)} \leq \overline{X}_j, \quad \forall k \tag{4.11}$$

$$B_{i\min}\overline{q}_i \leq \overline{B}_i \leq B_{i\max}\overline{q}_i \tag{4.12}$$

$$X_{j\min}\bar{q}_j \le \overline{X}_j \le X_{j\max}\bar{q}_j \tag{4.13}$$

$$\bar{q}_i, \bar{q}_j = 0,1 \tag{4.14}$$

The decision variables are $\overline{B}_i^{(k)}$, $\overline{B}_i$, $\bar{q}_i$, $\overline{X}_j^{(k)}$, $\overline{X}_j$ and $\bar{q}_j$.

Here,

- $\overline{B}_i$ is the new size of the switched shunt capacitor at location *i*,
- $\overline{X}_j$ is the new size of the switched series capacitor at location *j*,
- $\bar{q}_i$ and $\bar{q}_j$ are new binary control location variables,
- $\overline{S}_i^{(k)}$ is the updated sensitivity of the voltage stability margin with respect to the susceptance of the shunt capacitor at location *i* under contingency *k*,
- $\overline{S}_j^{(k)}$ is the updated sensitivity of the voltage stability margin with respect to the reactance of the series capacitor at location *j* under contingency *k*,
- $\overline{B}_i^{(k)}$ is the new size of the switched shunt capacitor at location *i* under contingency k,
- $\overline{X}_j^{(k)}$ is the new size of the switched series capacitor at location *j* under contingency k, and
- $\overline{M}^{(k)}$ is the updated voltage stability margin under contingency *k*.

The above successive MIP will end until all concerned contingencies have satisfactory voltage stability margin and there is no significant movement of the decision variables from the previous MIP solution.

4.3 Numerical Results

The proposed method has been applied to the New England 39-bus system. In the

simulations, the following conditions are implemented unless stated otherwise:

- Loads are modeled as constant power;
- In computing voltage stability margin, the power factor of the load bus remains constant when the load increases, and load and generation increase are proportional to their base case value;
- The system MVA base is 100;
- Required voltage stability margin is assumed to be 10%;
- The parameter values adopted in the optimization problem are given in Table 4.1.

Table 4.1 Parameter values in the optimization formulation

	Shunt capacitor	Series capacitor
Maximum size (p.u.)	1.5	70% compensation
Minimum size (p.u.)	$B_{imin}=10^{-3}$	$X_{jmin}=10^{-3}$

Considering all N-1 contingencies, using the fast contingency screening and CPF methods, there exist 3 contingencies that result in a post-contingency voltage stability margin less than 10% as shown in Table 4.2.

Table 4.2 Voltage stability margin under three moderate contingencies

Contingency	Voltage Stability Margin (%)
(1). Outage of the generator at bus 31	2.69
(2). Outage of the generator at bus 32	2.46
(3). Outage of the generator at bus 35	2.42

The candidate control locations are determined based on the linear search algorithm presented in Chapter 2. The best seven candidate buses to install switched shunt capacitors are buses 5, 6, 7, 10, 11, 12, and 13. The best eight candidate lines to install switched series capacitors are lines 2-3, 3-4, 4-5, 6-7, 8-9, 13-14, 15-16, and 16-19. For these candidate locations, the optimization based reactive power control planning algorithm presented in Sections III.E and III.F was carried out.

In order to demonstrate the efficacy of the proposed method, two cases are considered as follows. In case 1, only switched shunt capacitors are chosen as candidate controls while both switched shunt and switched series capacitors are chosen as candidate controls in case 2. Table 4.3 shows the results for case 1 where the optimal allocations for switched shunt capacitors are 0.747 p.u., 1.500 p.u., 0.866 p.u., 1.500 p.u. and 1.500 p.u. at buses 5, 6, 10, 11, and 12 respectively. The total cost is $ 9.006 million for the control allocations in case 1. On the other hand, the optimal control allocations for case 2 are shown in Table 4.4 indicating a switched series capacitor of 0.011 p.u. on line 2-3, a switched series capacitor of 0.025 p.u. on line 8-9 and a switched shunt capacitor of 0.973 p.u. at bus 12. For case 2, the total cost for control allocations is $ 7.326 million which is 18.7% less than that of case 1. This result shows that benefit can be obtained by coordinated planning of different types of discrete reactive power controls. Table 4.5 gives the verified results of the reactive power control planning with the continuation power flow program. Clearly, the voltage stability margins of the concerned contingencies are all increased to be greater than the required value of 10% under the planned controls. The iteration number in the second column represents the number of times of performing the MIP to get the optimal solution.

Table 4.3 Control allocations for shunt capacitors to increase voltage stability margin

Locations for shunt cap.	Maximum size Limit (p.u.)	Overall optimal control allocation (p.u.)	Solution to cont. (1) (p.u.)	Solution to cont. (2) (p.u.)	Solution to cont. (3) (p.u.)
Bus 5	1.500	0.747	0.747	0.747	0.747
Bus 6	1.500	1.500	1.384	1.500	1.500
Bus 10	1.500	0.866	0.866	0.866	0.866
Bus 11	1.500	1.500	1.500	1.500	1.500
Bus 12	1.500	1.500	1.500	1.500	1.500

Table 4.4 Control allocations for shunt and series capacitors to increase voltage stability margin

Locations for shunt and series cap.	Maximum size limit (p.u.)	Overall optimal control allocation (p.u.)	Solution to cont. (1) (p.u.)	Solution to cont. (2) (p.u.)	Solution to cont. (3) (p.u.)
Bus 12	1.500	0.973	0.258	0.361	0.973
Line 2-3	0.011	0.011	0.011	0.011	0.011
Line 8-9	0.025	0.025	0.025	0.025	0.025

Table 4.5 Voltage stability margin under planned controls

Candidate controls	Iteration number for MIP	Voltage stability margin for cont. (1)	Voltage stability margin for cont. (2)	Voltage stability margin for cont. (3)
Shunt capacitors	6	10.01%	10.01%	10.01%
Shunt and series capacitors	3	10.01%	10.01%	10.02%

4.4 Summary

This chapter presents an optimization based method of planning reactive power controls in electric transmission systems to satisfy the voltage stability margin requirement under a set of contingencies. The backward/forward search algorithm with linear complexity is used to select candidate locations for switched shunt and series capacitors. Optimal locations and amounts of new switch controls are obtained by solving a sequence of mixed integer

programming problems. The effectiveness of the method is illustrated using the New England 39 bus system. The results show that the method works satisfactorily to plan reactive power controls.

CHAPTER 5 OPTIMAL ALLOCATION OF STATIC AND DYNAMIC VAR RESOURCES

5.1 Introduction

Sufficient controllable reactive power resources are essential for reliable operation of electric power systems. Inadequate reactive power support has led to voltage collapses and has been a cause of several recent major power outages worldwide. While the August 2003 blackout in the United States and Canada was not due to a voltage collapse, the final report of the U.S.-Canada Power System Outage Task force said that "insufficient reactive power was an issue in the blackout" [67].

Generally, reactive power supply can be divided into two categories: static and dynamic VAR resources. Dynamic VAR resources such as Static VAR Compensators (SVCs) have a fast response time while static VAR resources such as Mechanically Switched Capacitors (MSCs) have a relatively slow response time [10]. In addition, dynamic VAR devices can continuously control reactive power output but static VAR devices can not. On the other hand, the cost of static VAR resources is much lower than that of dynamic VAR resources [24]. Differences in effectiveness and costs of different devices dictate that reactive power generally is provided by a mix of static and dynamic VAR resources. Mechanically switched capacitors are cost-effective to increase post-contingency voltage stability margin. More expensive SVCs are usually used to deal with transient voltage dip and short-term voltage stability problems [4, 61, 68, 69, 70, 71] because the capability for rapid on-off switching of mechanically switched capacitors is significantly limited [72]. In this chapter, we focus on mechanically switched shunt capacitors as static VAR resources and SVCs as dynamic VAR resources because they have been widely used in the electric power industry as reactive power

support. However, the proposed algorithm is applicable to plan other VAR resources as well.

There are three basic problems to be addressed for planning static and dynamic VAR resources:

1) how much reactive capacity to build;
2) where to build;
3) what should be split between static and dynamic VAR resources.

There is a limited amount of publications about coordinated planning of static and dynamic VAR resources. The methods in [42] [43] [44] [45] use a sequential procedure to allocate static and dynamic VAR resources. In this chapter, an optimization based method is presented to simultaneously determine the optimal allocation of static and dynamic VAR resources to satisfy the requirements of voltage stability margin and transient voltage dip. The remaining parts of this chapter are organized as follows. Section 5.2 presents transient voltage dip sensitivities. Section 5.3 describes the proposed mixed integer programming based method to optimally allocate static and dynamic VAR resources. Section 5.4 provides numerical results to illustrate the effectiveness of the approach. Section 5.5 concludes.

5.2 Transient Voltage Sensitivities

An SVC is an effective means to mitigate transient voltage dip by providing dynamic reactive power support. The ability of an SVC to mitigate transient voltage dip depends on the SVC's capacitive limit (size) B_{svc}, as shown in Figure 5.1. Dynamic reactive power support increases with B_{svc}, but so does the SVC cost. We desire to identify the most effective locations and to determine the minimum capacitive limits of SVCs such that the transient voltage dip criteria are satisfied. To do this, we deploy a sequence of linear search/optimizations which require voltage dip magnitude and duration sensitivities to the

SVC capacitive limit. These sensitivities are derived in this section.

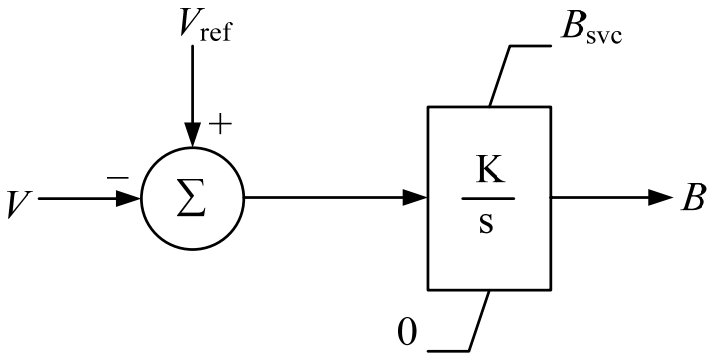

Figure 5.1 Static VAR compensator model

As shown in Figure 5.1, there is a non-windup limit on the SVC output, constraining the SVC susceptance output B. When the SVC output reaches the capacitive limit, the SVC becomes non-controllable and is equivalent to a shunt capacitor. Therefore, the power system model when the SVC output reaches the limit is different from that when the SVC output is within the limit. There are also hard limits on other power system controllers such as generator excitation systems [73]. Thus, the response of a power system is hybrid when studying large disturbances. It exhibits periods of smooth behavior, interspersed with discrete events. Smooth behavior is driven by devices such as generators and loads that are described by differential-algebraic equations. Discrete events are arising, for example, from enforcement of controller hard limits. Systems that exhibit intrinsic interactions between continuous dynamics and discrete events are generally called hybrid systems [74].

In order to derive the sensitivities of the voltage dip time duration and the maximum transient voltage dip to the SVC capacitive limit, the hybrid system nature of a power system need to be considered. The hybrid system model proposed in [73] and [75] is adopted here to derive the sensitivities. An overview of the hybrid system model is provided in Appendix A.

The sensitivities of the voltage dip time duration and the maximum transient voltage dip to the SVC capacitive limit are derived based on the trajectory sensitivities of hybrid systems presented in [75]. The trajectory sensitivities provide a way of quantifying the variation of a trajectory resulting from (small) changes to parameters and/or initial conditions [76]. An overview of the trajectory sensitivities is proved in Appendix B.

5.2.1 Sensitivity of Voltage Dip Time Duration to SVC Capacitive Limit

The sensitivity of the voltage dip time duration to the SVC capacitive limit is the change of the voltage dip time duration for a given change in the SVC capacitive limit which can be treated as a parameter and be included in x_0 which is a vector including parameters and initial conditions of state variables in Appendix B.

Let $\tau^{(1)}$ be the time at which the transient voltage dip begins after a fault is cleared and $\tau^{(2)}$ the time at which the transient voltage dip ends as shown in Figure 1.3 Then the time duration of the transient voltage dip τ_{dip} is given by

$$\tau_{\text{dip}} = \tau^{(2)} - \tau^{(1)} \tag{5.1}$$

Thus, the sensitivity of the voltage dip time duration to the capacitive limit of an SVC, S_τ, is

$$S_\tau \equiv \frac{\partial \tau_{dip}}{\partial B_{\text{svc}}} = \frac{\partial(\tau^{(2)} - \tau^{(1)})}{\partial B_{\text{svc}}} = \frac{\partial \tau^{(2)}}{\partial B_{\text{svc}}} - \frac{\partial \tau^{(1)}}{\partial B_{\text{svc}}} = \tau^{(2)}_{B_{\text{svc}}} - \tau^{(1)}_{B_{\text{svc}}} \tag{5.2}$$

where $\tau^{(1)}_{B_{\text{svc}}}$ and $\tau^{(2)}_{B_{\text{svc}}}$ are calculated in (B.9) of Appendix B. Note that the hypersurface $s(x,y)$ in (B.9) is defined by $0.8V_i(0) - V_i(t)$ when calculating $\tau^{(1)}_{B_{\text{svc}}}$, and is defined by $V_i(t) - 0.8V_i(0)$ when calculating $\tau^{(2)}_{B_{\text{svc}}}$ where V_i is the voltage at load bus i.

Bus voltage recovery may be slow after a fault is cleared as shown in Figure 5.2. In this case, $\tau^{(1)}$ is equal to the time at which the fault is cleared. Therefore, $\tau^{(1)}_{B_{\text{svc}}} = 0$ and $S_\tau = \tau^{(2)}_{B_{\text{svc}}}$.

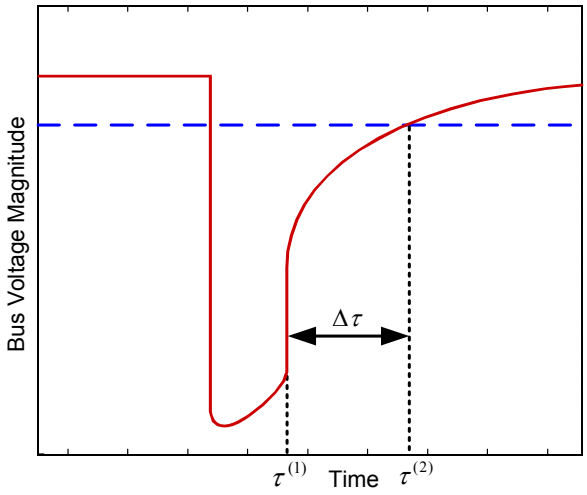

Figure 5.2 Slow voltage recovery after a fault

5.2.2 Sensitivity of Maximum Transient Voltage Dip to SVC Capacitive Limit

The maximum transient voltage dip V_{dip} after the fault is cleared is defined as

$$V_{\text{dip}} = \frac{V_0 - V_{\min}}{V_0} \times 100\% \tag{5.3}$$

where V_0 is the pre-fault voltage and $V_{\min}$ is the minimum voltage magnitude during the transient voltage dip.

The sensitivity of the maximum transient voltage dip to the SVC capacitive limit, S_V, is the change of the maximum transient voltage dip for a given change in the SVC capacitive limit

$$S_V \equiv \frac{\partial V_{dip}}{\partial B_{\text{svc}}} = -(\frac{\partial V_{\min}}{\partial B_{\text{svc}}})/V_0 = -(\frac{\partial V}{\partial B_{\text{svc}}}\Big|_{t=t_{\max\_\text{dip}}})/V_0 \tag{5.4}$$

where $\partial V/\partial B_{\text{svc}}$ is the voltage trajectory sensitivity to the SVC capacitive limit which is calculated by solving (B.3) and (B.4) in Appendix B, and $t_{\max\_\text{dip}}$ is the time when the maximum transient voltage dip (minimum voltage magnitude) occurs after the fault is cleared. Note that $t_{\max\_\text{dip}}$ is dependent upon B_{svc} and is obtained from the voltage trajectory where the rate of change of voltage is zero.

5.2.3 Numerical Approximation

From computation point of view, the trajectory sensitivities and the transient voltage dip sensitivities require the integration of a set of differential algebraic equations as shown in Appendix B. For large systems, these equations have high dimension. The computational cost of obtaining the sensitivities is minimal when an implicit numerical integration technique such as trapezoidal integration is used to generate the trajectory [75], [77], [78]. An alternative to calculate the sensitivities is using numerical approximation

$$S_{\tau} = \frac{\partial \tau_{\text{dip}}}{\partial B_{\text{svc}}} \approx \frac{\Delta \tau_{\text{dip}}}{\Delta B_{\text{svc}}} = \frac{\tau_{\text{dip}}(B_{\text{svc}} + \Delta B_{\text{svc}}) - \tau_{\text{dip}}(B_{\text{svc}})}{\Delta B_{\text{svc}}} \tag{5.5}$$

and

$$S_{V} = \frac{\partial V_{\text{dip}}}{\partial B_{\text{svc}}} \approx \frac{\Delta V_{\text{dip}}}{\Delta B_{\text{svc}}} = \frac{V_{\text{dip}}(B_{\text{svc}} + \Delta B_{\text{svc}}) - V_{\text{dip}}(B_{\text{svc}})}{\Delta B_{\text{svc}}} \tag{5.6}$$

The procedure requires repeated runs of simulation of the system model for the SVC capacitive limits B_{svc} and $B_{\text{svc}}+\Delta B_{\text{svc}}$. The senstivities are then given by the change of the voltage dip time duration or the maximum transient voltage dip divided by the SVC capacitive limit change ΔB_{svc}. The involved computational cost of this procedure may be greater than direct calculation of the sensitivities if many sensitivities are desired. However, it is easier to implement for a practical large power system. In this work, time domain simulations and voltage dip sensitivities were obtained using Siemens PTI's PSS/E^{TM} version 30.1 software.

5.3 Algorithm of Optimal Allocation of Static and Dynamic VAR Resources

A flowchart for planning static and dynamic VAR resources is shown in Figure 5.3. Each block in the flowchart will be explained in detail in the following subsections. After the contingency analysis, the proposed algorithm of allocation of static and dynamic VAR resources has three stages.

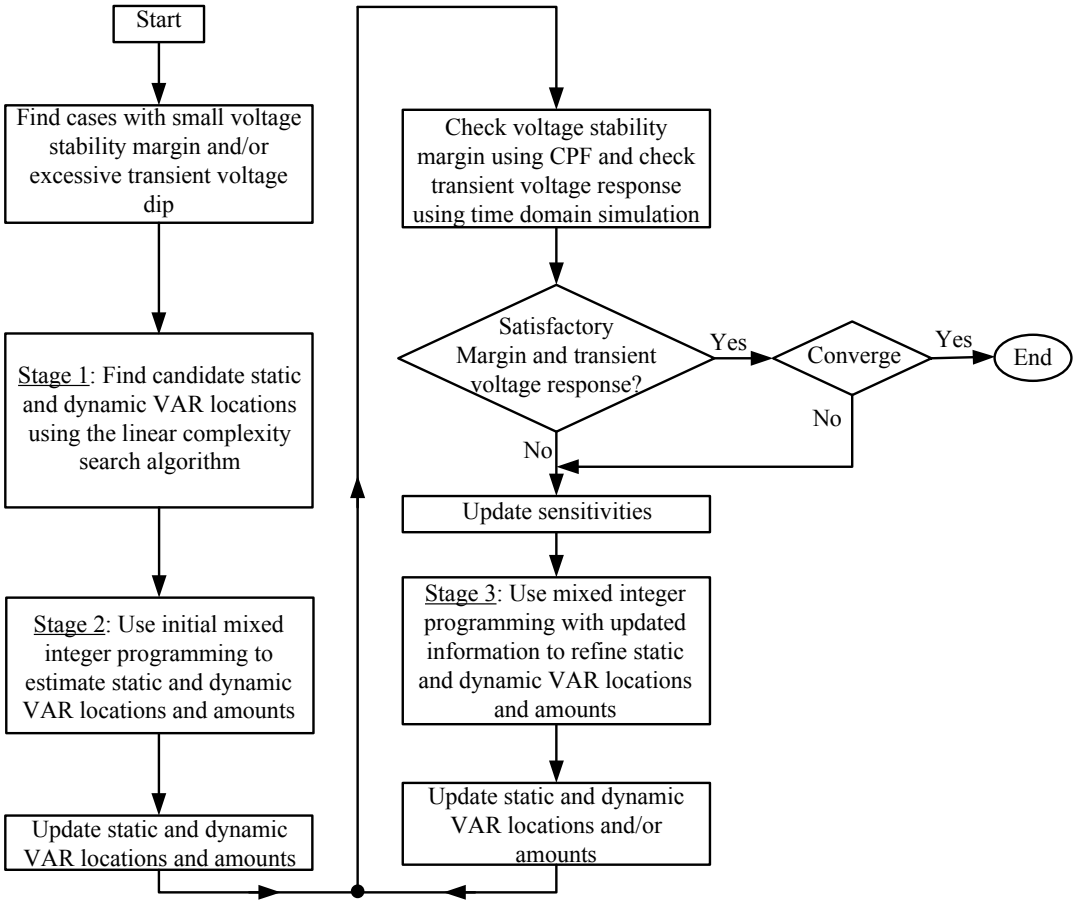

Figure 5.3 Flowchart for the static and dynamic VAR allocation

5.3.1 Contingency Analysis

In this step, the contingencies which cause insufficient voltage stability margin and/or excessive transient voltage dip problems are identified. In finding the contingencies having insufficient voltage stability margin, the fast contingency screening technique proposed in [55] is used. First, the post fault voltage stability margin is estimated based on voltage stability margin sensitivities. Then, the contingencies are ranked from most severe to least severe according to the value of the estimated voltage stability margin. After the ordered contingency list is obtained, each contingency is evaluated starting from the most severe one using the

continuation power flow. Evaluation terminates after encountering a certain number of sequential contingencies having the voltage stability margin greater than or equal to the required value, where the number depends on the size of the contingency list.

In finding the contingencies having excessive transient voltage dip problems, the time domain simulation is used. A program was developed to automate identification of contingencies and buses which violate the transient voltage dip criteria based on the output of the time domain simulation.

5.3.2 Selection of Candidate VAR Locations

An important step in the VAR planning problem is the selection of candidate locations. Candidate locations may be chosen based on experience and/or the relative value of linear sensitivities of new reactive power compensation devices. In this case, however, there is no guarantee that the selected candidate locations for reactive compensation are sufficient to satisfy the requirements of voltage stability margin and transient voltage dip. On the other hand, the computational cost to solve the Stage 2 mixed integer programming problem is high if all buses in a large power system are selected as candidates. To identify a sufficient but not excessive number of locations, the backward/forward search algorithm with linear complexity proposed in Chapter 2 can be used to find candidate locations for switched shunt capacitors and SVCs to increase voltage stability margin, and to find candidate locations for SVCs to deal with transient voltage dip problems. It is assumed that the capacities of switched shunt capacitors and SVCs are fixed at the maximum allowable value in this step.

5.3.3 Formulation of Initial Mixed Integer Programming

In stage 1, we find the candidate locations for mechanically switched shunt capacitors and SVCs. A mixed integer program (MIP) is used in stage 2 to exclude candidate locations not

needed, and to estimate the mix of mechanically switched shunt capacitors and SVCs at needed locations. The MIP minimizes the total installation cost of mechanically switched shunt capacitors and SVCs while satisfying the requirements of voltage stability margin and transient voltage dip.

minimize

$$J = \sum_{i\in\Omega}[C_{vi\_\text{shunt}}B_{i\_\text{shunt}} + C_{fi\_\text{shunt}}q_{i\_\text{shunt}} + C_{vi\_\text{svc}}B_{i\_\text{svc}} + C_{fi\_\text{svc}}q_{i\_\text{svc}}] \tag{5.7}$$

subject to

$$\sum_{i\in\Omega} S_{M,i}^{(k)}[B_{i\_\text{shunt}}^{(k)} + B_{i\_\text{svc}}^{(k)}] + M^{(k)} \geq M_{\text{r}}, \forall k \tag{5.8}$$

$$\sum_{i\in\Omega_{\text{svc}}} S_{\tau,n,i}^{(k)}B_{i\_\text{svc}}^{(k)} + \tau_{\text{dip},n}^{(k)} \leq \tau_{\text{dip},n,\text{r}}, \forall n,k \tag{5.9}$$

$$\sum_{i\in\Omega_{\text{svc}}} S_{V,n,i}^{(k)}B_{i\_\text{svc}}^{(k)} + V_{\text{dip},n}^{(k)} \leq V_{\text{dip},n,\text{r}}, \forall n,k \tag{5.10}$$

$$B_{i\,\text{min\_shunt}} \leq B_{i\_\text{shunt}}^{(k)} \leq B_{i\_\text{shunt}}, \forall k \tag{5.11}$$

$$B_{i\,\text{min\_svc}} \leq B_{i\_\text{svc}}^{(k)} \leq B_{i\_\text{svc}}, \forall k \tag{5.12}$$

$$B_{i\,\text{min\_shunt}}q_{i\_\text{shunt}} \leq B_{i\_\text{shunt}} \leq B_{i\,\text{max\_shunt}}q_{i\_\text{shunt}} \tag{5.13}$$

$$B_{i\,\text{min\_svc}}q_{i\_\text{svc}} \leq B_{i\_\text{svc}} \leq B_{i\,\text{max\_svc}}q_{i\_\text{svc}} \tag{5.14}$$

$$q_{i\_\text{shunt}}, q_{i\_\text{svc}} = 0,1 \tag{5.15}$$

The decision variables are $B_{i\_\text{shunt}}^{(k)}$, B_{i_shunt}, q_{i_shunt}, $B_{i\_\text{svc}}^{(k)}$, B_{i_svc}, and q_{i_svc}.

Variable definition follows:

- C_{f_shunt} is fixed installation cost and C_{v_shunt} is variable cost of shunt capacitors,
- C_{f_svc} is fixed installation cost and C_{v_svc} is variable cost of SVCs,
- B_{i_shunt}: size of the shunt capacitor at location i,
- B_{i_svc}: size of the SVC at location i,
- q_{i_shunt}=1 if the location i is selected for installing shunt capacitors, otherwise, q_{i_shunt}=0,
- q_{i_svc}=1 if the location i is selected for installing SVCs, otherwise, q_{i_svc}=0,

- the superscript k represents the contingency causing insufficient voltage stability margin and/or excessive transient voltage dip problems,
- Ω_{shunt}: set of candidate locations to install shunt capacitors,
- Ω_{svc}: set of candidate locations to install SVCs,
- Ω: union of Ω_{shunt} and Ω_{svc},
- $B_{i\_shunt}^{(k)}$: size of the shunt capacitor to be switched on at location i under contingency k,
- $B_{i\_svc}^{(k)}$: size of the SVC at location i under contingency k,
- $S_{M,i}^{(k)}$: sensitivity of the voltage stability margin with respect to the shunt susceptance at location i under contingency k,
- $S_{\tau,n,i}^{(k)}$: sensitivity of the voltage dip time duration at bus n with respect to the size of the SVC at location i under contingency k,
- $S_{V,n,i}^{(k)}$: sensitivity of the maximum transient voltage dip at bus n with respect to the size of the SVC at location i under contingency k,
- $M^{(k)}$: voltage stability margin under contingency k and without controls,
- M_r: required voltage stability margin,
- $\tau_{dip,n}^{(k)}$: time duration of voltage dip at bus n under contingency k and without controls,
- $\tau_{dip,n,r}$: maximum allowable time duration of voltage dip at bus n,
- $V_{dip,n}^{(k)}$: maximum transient voltage dip at bus n under contingency k and without controls,
- $V_{dip,n,r}$: maximum allowable transient voltage dip at bus n,
- $B_{i\min\_shunt}$: minimum size of the shunt capacitor at location i,

- $B_{i\max\_shunt}$: maximum size of the shunt capacitor at location i,
- $B_{i\min\_svc}$: minimum size of the SVC at location i, and
- $B_{i\max\_svc}$: maximum size of the SVC at location i.

The inequality constraint in (5.8) requires that the voltage stability margin under each concerned contingency is greater than the required value. Note that SVCs can also be used to increase the voltage stability margin. The inequality constraint in (5.9) requires that the time duration of transient voltage dip for each concerned bus under each concerned contingency is less than the maximum allowable value. The inequality constraint in (5.10) requires that the maximum transient voltage dip for each concerned bus under each concerned contingency is less than the maximum allowable value.

The optimization formulation in (5.7)-(5.15) does not directly involve complex steady state and dynamic power system models. Instead, it uses the corresponding sensitivity information. In addition, the backward/forward search algorithm provides that the number of candidate locations for reactive compensation can be limited to be relatively small even for problems of the size associated with practical power systems. Therefore, the computational cost for solving the above mixed integer programming formulation is not high even for large-scale power systems. The branch-and-bound method is used to solve this mixed integer programming problem.

The output of the mixed integer programming problem is the reactive compensation locations and amounts for all concerned contingencies and the combined reactive compensation location and amount. Then the network configuration is updated by including the identified reactive power support under each contingency. After that, the voltage stability margin is recalculated using CPF to check if sufficient margin is achieved for each concerned

contingency. Also, time domain simulations are carried out to check whether the requirement of the transient voltage dip performance is met. This step is necessary because the power system model is inherently nonlinear, and the mixed integer programming algorithm uses linear sensitivities to estimate the effect of variations of reactive support levels on the voltage stability margin and transient voltage dip. As a result, there may be contingencies that have insufficient voltage stability margin or excessive transient voltage dip after updating the network configuration according to results of the initial mixed integer programming problem. Also, the obtained solution may not be optimal after one iteration of MIP. The reactive compensation locations and/or amounts can be further refined by recomputing sensitivities (with updated network configuration) under each concerned contingency, and solving a second-stage mixed integer programming problem, as described in the next subsection.

5.3.4 Formulation of MIP with Updated Information

The successive MIP problem is formulated to minimize the total installation cost of mechanically switched shunt capacitors and SVCs subject to the constraints of the requirements of voltage stability margin and transient voltage dip, as follows:

minimize

$$J = \sum_{i\in\Omega}[C_{vi\_\text{shunt}}\overline{B}_{i\_\text{shunt}} + C_{fi\_\text{shunt}}\overline{q}_{i\_\text{shunt}} + C_{vi\_\text{svc}}\overline{B}_{i\_\text{svc}} + C_{fi\_\text{svc}}\overline{q}_{i\_\text{svc}}] \tag{5.16}$$

subject to

$$\sum_{i\in\Omega}\overline{S}_{M,i}^{(k)}[(\overline{B}_{i\_\text{shunt}}^{(k)} - B_{i\_\text{shunt}}^{(k)}) + (\overline{B}_{i\_\text{svc}}^{(k)} - B_{i\_\text{svc}}^{(k)})] + \overline{M}^{(k)} \geq M_{\text{r}},\ \forall k \tag{5.17}$$

$$\sum_{i\in\Omega_{svc}}\overline{S}_{\tau,n,i}^{(k)}(\overline{B}_{i\_\text{svc}}^{(k)} - B_{i\_\text{svc}}^{(k)}) + \overline{\tau}_{\text{dip},n}^{(k)} \leq \tau_{\text{dip},n,\text{r}},\ \forall n,k \tag{5.18}$$

$$\sum_{i\in\Omega_{svc}}\overline{S}_{V,n,i}^{(k)}(\overline{B}_{i\_\text{svc}}^{(k)} - B_{i\_\text{svc}}^{(k)}) + \overline{V}_{\text{dip},n}^{(k)} \leq V_{\text{dip},n,\text{r}},\ \forall n,k \tag{5.19}$$

$$B_{i\,\text{min\_shunt}} \leq \overline{B}_{i\_\text{shunt}}^{(k)} \leq \overline{B}_{i\_\text{shunt}},\ \forall k \tag{5.20}$$

$$B_{i\min\_svc} \le \overline{B}_{i\_svc}^{(k)} \le \overline{B}_{i\_svc}, \forall k \tag{5.21}$$

$$B_{i\min\_shunt}\overline{q}_{i\_shunt} \le \overline{B}_{i\_shunt} \le B_{i\max\_shunt}\overline{q}_{i\_shunt} \tag{5.22}$$

$$B_{i\min\_svc}\overline{q}_{i\_svc} \le \overline{B}_{i\_svc} \le B_{i\max\_svc}\overline{q}_{i\_svc} \tag{5.23}$$

$$\overline{q}_{i\_shunt}, \overline{q}_{i\_svc} = 0,1 \tag{5.24}$$

The decision variables are $\overline{B}_{i\_shunt}^{(k)}$, $\overline{B}_{i\_shunt}$, $\overline{q}_{i\_shunt}$, $\overline{B}_{i\_svc}^{(k)}$, $\overline{B}_{i\_svc}$ and $\overline{q}_{i\_svc}$.

Variable definition follows:

- $\overline{B}_{i\_shunt}$: new size of the shunt capacitor at location *i*,
- $\overline{B}_{i\_svc}$: new size of the SVC at location *i*,
- $\overline{q}_{i\_shunt}$ and $\overline{q}_{i\_svc}$ are new binary location variables for shunt capacitors and SVCs,
- $\overline{S}_{M,i}^{(k)}$: updated sensitivity of the voltage stability margin with respect to the shunt susceptance at location *i* under contingency *k*,
- $\overline{S}_{\tau,n,i}^{(k)}$: updated sensitivity of the voltage dip time duration at bus *n* with respect to the size of the SVC at location *i* under contingency *k*,
- $\overline{S}_{V,n,i}^{(k)}$: updated sensitivity of the maximum transient voltage dip at bus *n* with respect to the size of the SVC at location *i* under contingency *k*,
- $\overline{B}_{i\_shunt}^{(k)}$: new size of the shunt capacitor at location *i* under contingency *k*,
- $\overline{B}_{i\_svc}^{(k)}$: new size of the SVC at location *i* under contingency *k*,
- $\overline{M}^{(k)}$: updated voltage stability margin under contingency *k*,
- $\overline{\tau}_{\mathrm{dip},n}^{(k)}$: updated time duration of voltage dip at bus *n* under contingency *k*, and
- $\overline{V}_{\mathrm{dip},n}^{(k)}$: updated maximum transient voltage dip at bus *n* under contingency *k*.

The inequalities in (5.17)-(5.19) are the constraints of voltage stability margin, time duration of voltage dip and the maximum transient voltage dip respectively. They incorporate

updated sensitivities, voltage stability margin and transient voltage dip behavior under each concerned contingency. The above successive MIP will end until all concerned contingencies have satisfactory voltage stability margin and transient voltage response and there is no significant movement of the decision variables from the previous MIP solution.

5.4 Numerical Results

The proposed method has been applied to the New England 39 bus system, In the simulations, the following conditions are implemented unless stated otherwise:

- The required voltage stability margin is assumed to be 10%;
- The WECC reliability criteria is adopted for transient voltage dip problems;
- In computing voltage stability margin and margin sensitivities, 1) loads are modeled as constant power, 2) reactive power output limits of generators are modeled, 3) the power factor of the load remains constant when the load increases, and load and generation increase are proportional to their base case value;
- In performing time domain simulations and calculating the transient voltage dip sensitivities, loads are modeled as 30% constant impedance, 30% constant current and 40% constant power;
- The parameter values adopted in the optimization problem are given in Table 5.1.

Table 5.1 Parameter values adopted in optimization problem

	Shunt capacitor	SVC
Variable cost ($ million/100 Mvar)	0.41	5
Fixed cost ($ million)	1.3	1.5
Maximum size (p.u.)	1.0	1.0
Minimum size (p.u.)	10^{-3}	10^{-3}

Two contingencies violating reliability criteria are considered to illustrate the proposed algorithm of optimal allocating static and dynamic VAR resources. The first contingency is outage of the generator at bus 31. The second contingency is a three-phase-to-ground short-circuit fault on the transmission line 5-6, followed by clearance of the fault by removal of the transmission line. The details of the two contingencies are listed in Table 5.2. The first contingency violates the voltage stability margin criteria while the second contingency violates the transient voltage dip criteria at the load bus 7.

Table 5.2 Contingencies violating reliability criteria

Contingency	Voltage stability margin (%)	Time duration of voltage dip exceeding 20% (cycles)	Maximum transient voltage dip (%)
(1). Outage of the generator at bus 31	2.69	No violation	No violation
(2). Short circuit and outage of the line 5-6 (voltage at load bus 7)	No violation	29.10	26.83

The candidate control locations are determined based on the linear search algorithm presented in Section 5.3.2. Six candidate buses are chosen to install switched shunt capacitors and SVCs. They are buses 6, 7, 8, 10, 11 and 12. For these candidate locations, the optimization based reactive power planning algorithm presented in Sections 5.3.3 and 5.3.4 was carried out. Table 5.3 shows the allocation of mechanically switched shunt capacitors as 1.0 p.u., 0.178 p.u., 1.0 p.u., 1.0 p.u., 1.0 p.u. at buses 6, 7, 10, 11, 12 respectively. These capacitors will be switched on under contingency 1 to increase the voltage stability margin. Table 5.4 shows the allocation of SVCs as 0.6 p.u., 1.0 p.u. at buses 6 and 7 respectively. The identified SVCs can eliminate the transient voltage dip problem under contingency 2. The

SVCs along with the switched shunt capacitors can increase the voltage stability margin to 10% under contingency 1. Table 5.5 shows that the requirements of voltage stability margin and transient voltage dip are satisfied with the planned static and dynamic VAR resources under the concerned two contingencies. Figure 5.4 shows the voltage responses at bus 7 under contingency 2 with and without SVCs. Figure 5.5 shows the SVC output at bus 6 under contingency 2. Figure 5.6 shows the SVC output at bus 7 under contingency 2. The outputs of both SVCs reach the capacitive limits during the transient voltage dip.

Table 5.3 Allocation of mechanically switched shunt capacitors

Locations for shunt cap.	Maximum size limit (p.u.)	Overall optimal control allocation (p.u.)	Solution to cont. (1) (p.u.)	Solution to cont. (2) (p.u.)
Bus 6	1.0	1	1	N/A
Bus 7	1.0	0.178	0.178	N/A
Bus 8	1.0	0	0	N/A
Bus 10	1.0	1	1	N/A
Bus 11	1.0	1	1	N/A
Bus 12	1.0	1	1	N/A

Table 5.4 Allocation of SVCs

Locations for SVC	Maximum size limit (p.u.)	Overall optimal control allocation (p.u.)	Solution to cont. (1) (p.u.)	Solution to cont. (2) (p.u.)
Bus 6	1.0	0.6	0.6	0.6
Bus 7	1.0	1.0	1.0	1.0
Bus 8	1.0	0	0	0
Bus 10	1.0	0	0	0
Bus 11	1.0	0	0	0
Bus 12	1.0	0	0	0

Table 5.5 System performance under planned static and dynamic VARs

Contingency	Voltage stability margin (%)	Time duration of voltage dip exceeding 20% (cycles)	Maximum transient voltage dip (%)
(1). Outage of the generator at bus 31	10.02%	No violation	No violation
(2). Short circuit and outage of the line 5-6 (voltage at load bus 7)	No violation	20	23.74

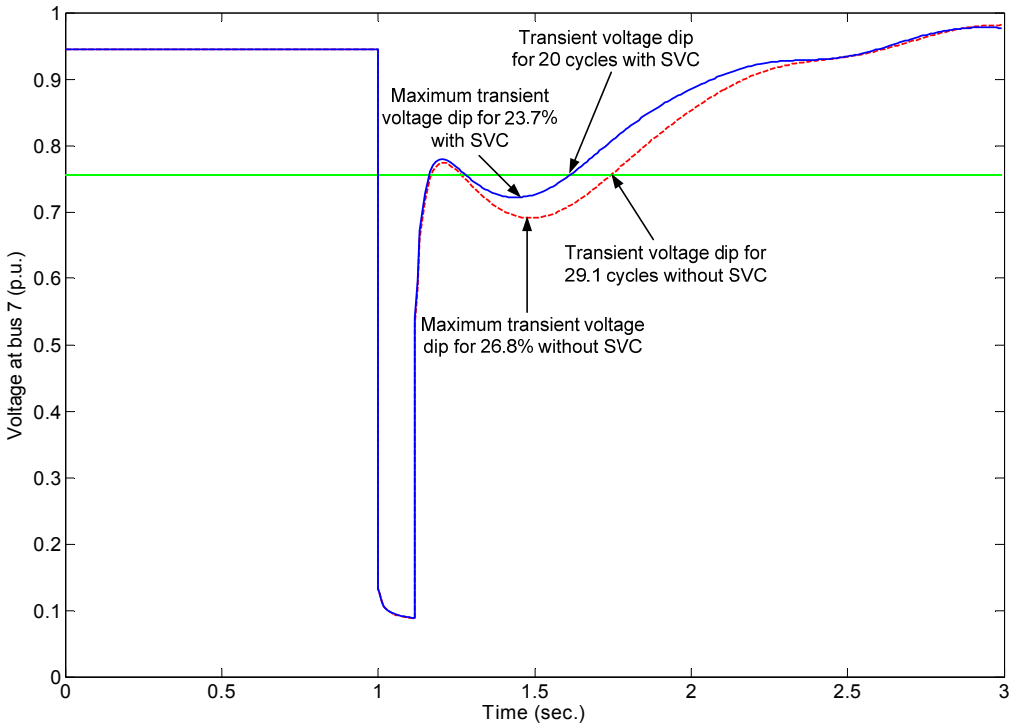

Figure 5.4 Voltage response at bus 7 under contingency 2

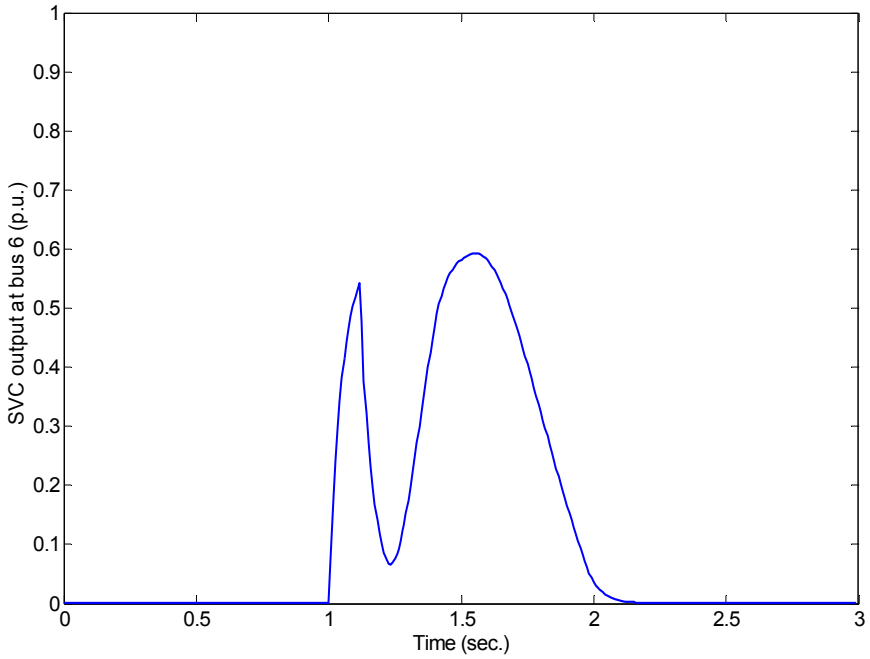

Figure 5.5 SVC output at bus 6 under contingency 2

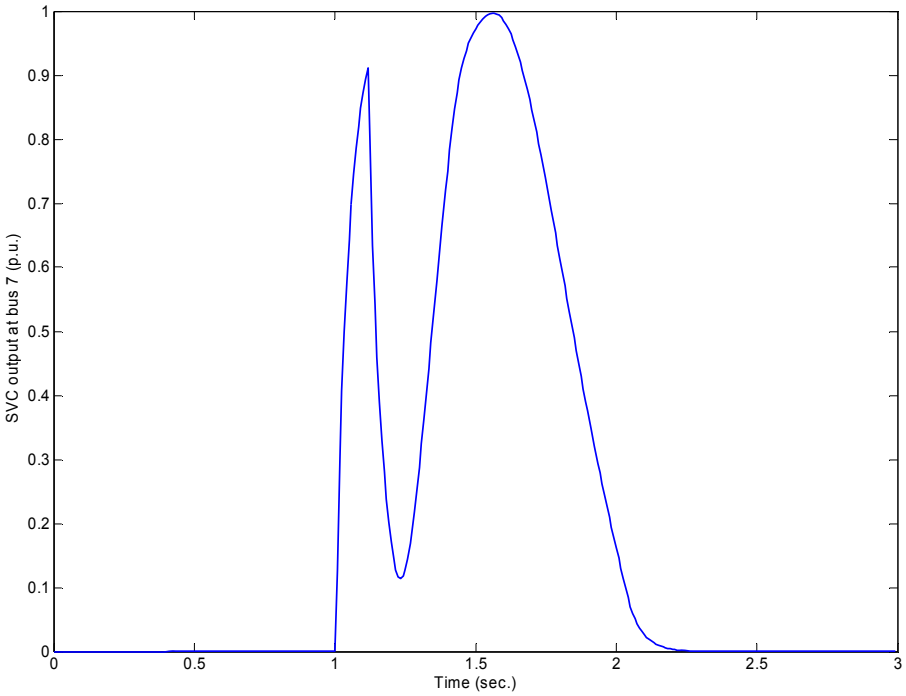

Figure 5.6 SVC output at bus 7 under contingency 2

5.5 Summary

This chapter presents an optimization based method of coordinated planning of static and dynamic VAR resources in electric transmission systems to satisfy the requirements of voltage stability margin and transient voltage dip under contingencies. The backward/forward search algorithm with linear complexity is used to select candidate locations for VAR resources. Optimal locations and amounts of new VAR resources are obtained by solving a sequence of mixed integer programming problems. The effectiveness of the method is illustrated using the New England 39 bus system. The results show that the method works satisfactorily to plan static and dynamic VAR resources under a set of contingencies.

CHAPTER 6 CONCLUSTIONS AND FUTURE WORK

6.1 Conclusions

This dissertation developed systematic algorithms to plan reactive power controls for transmission enhancement. The research has been motivated by recent major power outages worldwide caused by voltage instability and the industry need of effective algorithms of reactive power control planning to counteract voltage instability and thus enhance the electric transmission system. The main contributions of this research are the development of algorithms to select candidate control locations to satisfy system performance requirements, the derivation of transient voltage dip sensitivities for dynamic VAR planning, and the development of reactive power control planning algorithms to restore post-contingency equilibria, to increase post-contingency voltage stability margin, and to mitigate post-contingency transient voltage dip. All the proposed algorithms have been implemented with MATLAB and tested on the New England 39-bus system. The simulation results indicate that they can be used to effectively plan reactive power controls for electric transmission system enhancement.

The specific contributions of this research are summarized as follows:

1. Development of a backward/forward search algorithm to select candidate locations of reactive power controls while satisfying power system performance requirements. In the past, candidate control locations are usually chosen based on the engineering judgment. There is no guarantee that the selected locations are effective and sufficient to provide required reactive power support for all concerned contingencies. The proposed algorithm, however, can identify effective

and sufficient candidate locations for reactive power control planning. It reduces the computational cost to solve the MIP/MINLP based reactive power control planning problem by limiting the number of candidate locations. It has complexity linear in the number of feasible reactive power control locations whereas the solution space is exponential. Simulation results show that the backward/forward search algorithm can effectively find candidate reactive power control locations.

2. Development of a mixed integer programming based algorithm of reactive power control planning to restore equilibria under a set of severe contingencies. In the past, optimal power flow techniques could be used to restore post-contingency equilibrium for each contingency. It is hard to solve the conventional OPF problems considering multiple contingencies at the same time since they need to incorporate the power system models for all the concerned contingencies. However, it is very easy for the proposed algorithm to handle multiple contingencies. It is only in calculating the critical points and associated sensitivities that we must deal with the full size of the power system. Simulation results indicate that this algorithm is effective and fast to find good reactive power controls for the restoration of post-contingency equilibria.
3. Development of a mixed integer programming based algorithm of reactive power control planning to increase voltage stability margin under a set of contingencies. Again, the proposed algorithm is very effective in dealing with voltage stability requirements under multiple contingencies compared with conventional methods. Because the optimization formulation is linear, it is fast, yet it provides good solutions for large-scale power systems compared with MINLP. Simulation results

show that this algorithm is effective to plan reactive power controls for the increase of the post-contingency voltage stability margin.

4. Development of a systematic algorithm of coordinated planning of static and dynamic VAR resources while satisfying the performance requirements of voltage stability margin and transient voltage dip. It is the first time to use the optimization based method for the determination of the optimal balance between static and dynamic VAR resources. This work is also the first to propose the use of transient voltage dip sensitivities for dynamic VAR planning. Simulation results indicate that the proposed algorithm is effective to determine the optimal mix of static and dynamic VAR resources. The total installation cost of reactive power control devices can be reduced by using the proposed simultaneous optimization formulation.

6.2 Future Work

In the future work, the following issues should be addressed:

1. Consideration of other stability/security constraints. This research has focused on the reactive power control planning to increase the voltage stability margin and to mitigate the transient voltage dip. Other stability/security constraints such as transient stability and post-contingency bus voltage magnitude requirements may also be included in the optimization formulation of the reactive power control planning.
2. Economic benefit analysis and cost allocation. The planned reactive power control devices are intended to serve as control response for contingencies. Further research on quantifying the economic benefit of these devices and efficiently

allocating the investment cost under the environment of deregulation is challenging but important.

APPENDIX A HYBRID SYSTEM MODEL

Without any discrete event, a power system can be described by a set of differential algebraic equations

$$\dot{x} = f(x, y) \tag{A.1}$$

$$0 = g(x, y) \tag{A.2}$$

with the vectors

$$x = \begin{bmatrix} x \\ p \end{bmatrix}, \quad f = \begin{bmatrix} f \\ 0 \end{bmatrix} \tag{A.3}$$

where $\underline{x} \in R^n$ are true dynamic states, $p \in R^l$ are parameters, $y \in R^m$ are algebraic states. Incorporating parameters into dynamic states allows a compact development of trajectory sensitivities in Appendix B.

Switching events, such as network topology changing, will alter the algebraic equations in (A.2) as

$$0 = \begin{cases} g^-(x, y) & s(x, y) < 0 \\ g^+(x, y) & s(x, y) > 0 \end{cases} \tag{A.4}$$

where $g^-(x,y)$ and $g^+(x,y)$ are sets of algebraic equations before and after the triggering event respectively, $s(x,y)$ is the triggering function. After the triggering event, algebraic variables y may have a step change in order to satisfy the new algebraic constraints.

Other event, such as transformer tap changing, can be modeled by a reset equation

$$x^+ = h(x^-, y^-) \qquad s(x, y) = 0 \tag{A.5}$$

with the vector

$$h = \begin{bmatrix} \underline{h} \\ p \end{bmatrix} \tag{A.6}$$

where $\underline{h}$ is the reset function of the dynamic states $\underline{x}$. Reset events (A.5) cause a discrete change in elements of $\underline{x}$.

The flows of x and y are defined as

$$x(t) = \phi_x(x_0, t) \tag{A.7}$$

$$y(t) = \phi_y(x_0, t) \tag{A.8}$$

with initial conditions,

$$\phi_x(x_0, t_0) = x_0 \tag{A.9}$$

$$g(x_0, \phi_y(x_0, t_0)) = 0 \tag{A.10}$$

More details of the above model can be found in [73] and [75].

APPENDIX B TRAJECTORY SENSITIVITIES

Changes of the flows ϕ_x and ϕ_y causing by deviations of the initial conditions and/or parameters are obtained by a Taylor series expansion of (A.7) and (A.8) and neglecting higher order terms

$$\Delta x(t) = \frac{\partial x(t)}{\partial x_0}\Delta x_0 \equiv \Phi_x(x_0,t)\Delta x_0 \tag{B.1}$$

$$\Delta y(t) = \frac{\partial y(t)}{\partial x_0}\Delta x_0 \equiv \Phi_y(x_0,t)\Delta x_0 \tag{B.2}$$

where Φ_x and Φ_y are the trajectory sensitivities [76].

The variational equations describing the evolution of trajectory sensitivities away from discrete events are obtained by differentiating (A.1) and (A.2) with respect to x_0

$$\dot{\Phi}_x = f_x(t)\Phi_x + f_y(t)\Phi_y \tag{B.3}$$

$$0 = g_x(t)\Phi_x + g_y(t)\Phi_y \tag{B.4}$$

Initial conditions for Φ_x and Φ_y are obtained from (A.9) and (B.4) as

$$\Phi_x(x_0,t_0) = I \tag{B.5}$$

$$0 = g_x(t_0) + g_y(t_0)\Phi_y(x_0,t_0) \tag{B.6}$$

The trajectory sensitivities are often discontinuous at a discrete event. The step changes in Φ_x and Φ_y are described by the jump conditions which also provide the initial conditions for the post-event evolution of trajectory sensitivities. Assume the trajectory crosses the hypersurface $s(x,y)=0$ at the point $(x(\tau),y(\tau))$. This point is called the junction point and τ is the junction time. The jump conditions for the sensitivities Φ_x are given by

$$\Phi_x(x_0,\tau^+) = h_x^*\Phi_x(x_0,\tau^-) - (f^+ - h_x^* f^-)\tau_{x0} \tag{B.7}$$

where

$$h_x^* = (h_x - h_y(g_y^-)^{-1} g_x^-)\,|_{\tau^-} \tag{B.8}$$

$$\tau_{x_0} = \frac{d\tau}{dx_0}(\tau^-) = -\frac{(s_x - s_y(g_y^-)^{-1} g_x^-)\,|_{\tau^-}\ \Phi_x(x_0, \tau^-)}{(s_x - s_y(g_y^-)^{-1} g_x^-)\,|_{\tau^-}\ f^-} \tag{B.9}$$

$$f^- \equiv f(x(\tau^-), y^-(\tau^-)) \tag{B.10}$$

$$f^+ \equiv f(x(\tau^+), y^+(\tau^+)) \tag{B.11}$$

Equation (B.9) describes the sensitivity of the junction time τ to the initial conditions and parameters. The sensitivities Φ_y are given by

$$\Phi_y(x_0, \tau^+) = -(g_y^+(\tau^+))^{-1} g_x^+(\tau^+)\Phi_x(x_0, \tau^+) \tag{B.12}$$

More details about derivation and numerical solution approaches for trajectory sensitivities can be found in [73] and [75].

REFERENCES

[1] L. Dale, “Reactive compensation using static VAR compensators-a planning case study using security constrained techniques,” in *Proc. International Conference on AC and DC Power Transmission*, Sept. 1991, pp. 50 – 54.

[2] R. Koessler, J. Mountford, L. Lima, and J. Rosende, “The Brazilian interconnected system: a study on transfer limits, reactive compensation and voltage collapse,” in *Proc. of the IEEE Power Engineering Society Winter Meeting*, Jan. 2001, pp. 1147 – 1153.

[3] P. Pourbeik, R. Koessler, and B. Ray, “Tools and techniques for analyzing voltage stability related reliability challenges,” in *Proc. of the IEEE Power Engineering Society Transmission and Distribution Conference and Exposition*, Sept. 2003, pp. 417 – 421.

[4] A. Hammad and M. El-Sadek, “Prevention of transient voltage instabilities due to induction motor loads by static VAr compensators,” *IEEE Trans. Power Syst.*, Vol. 4, pp. 1182 – 1190, Aug. 1989.

[5] X. Wang and J. R. McDonald, *Modern Power System Planning*. New York: McGraw Hill, 1994.

[6] IEEE/CIGRE joint task force on stability terms and definitions, “Definition and classification of power system stability”, *IEEE Trans. Power Syst*., vol. 19, pp. 1387-1401, Aug. 2004.

[7] U.G. Knight, *Power System in Emergencies from Contingency Planning to Crisis Management*. Chichester: John Wiley & Sons Ltd, 2001.

[8] NERC (North American Electric Reliability Corporation) Disturbance Analysis Working Group. Disturbances, load reductions, and unusual occurrences 1984-2002. [Online]. Available: http://www.nerc.com/~dawg/database.html (Date accessed: Mar. 9, 2007).

[9] Western Electricity Coordinating Council. NERC/WECC planning standards (Apr., 2005). [Online]. Available: http://www.wecc.biz/documents/library/procedures/CriteriaMaster.pdf (Date accessed: Mar. 9, 2007).

[10] T. Van Cutsem and C. Vournas, *Voltage Stability of Electric Power Systems*. Boston: Kluwer Academic Publishers, 1998.

[11] IEC 61000-4-30 "Electromagnetic Compatibility (EMC) – Part 4-30: Testing and Measurement Techniques – Power Quality Measurement Methods," Feb. 2003.

[12] D. J. Shoup, J. J. Paserba, C. W. Taylor, "A survey of current practices for transient voltage dip/sag criteria related to power system stability," in *Proc. of the IEEE Power Engineering Society Power Systems Conference and Exposition*, Oct. 2004, pp. 1140-1147.

[13] N. G. Hingorani and L. Gyugyi, *Understanding FACTS: Concepts and Technology of Flexible AC Transmission Systems*. New York: IEEE Press, 2000.

[14] "System protection schemes in power networks," CIGRE Publication, CIGRE Task Force 38-02-19, 2001.

[15] E. W. Kimbark, "Improvement of system stability by switched series capacitors," *IEEE Trans. Power Apparatus and Systems*, vol. PAS-85, pp. 180–188, Feb. 1966.

[16] W. Mittelstadt, C. W. Taylor, M. Klinger, J. Luini, J. D. McCalley, and J. Mechenbier, "Voltage instability modeling and solutions as applied to the Pacific Intertie," in *CIGRE Proc.*, chapter 38-230, 1990.

[17] P. M. Anderson and R. G. Farmer, *Series Compensation of Power Systems*. Encinitas: PBLSH! Inc., 1996.

[18] C. W. Taylor and A. L. Van Leuven, "CAPS: improving power system stability using the time-overvoltage capability of large shunt capacitor banks," *IEEE Trans. Power Delivery*, vol. 11, pp. 783–789, Apr. 1996.

[19] WECC. Emergency reporting and restoration procedures. [Online]. Available: http://www.wecc.biz/documents/library/RCS/RC001_Emerg_Reporting%204-21-04_WO%20diagrams.pdf (Date accessed: Mar. 9, 2007).

[20] C. W. Taylor, D. C. Erickson, K. E. Martin, R. E. Wilson, and V. Venkatasubramanian, "WACS - wide-area stability and voltage control systems: R&D and online demonstration," *Proc. IEEE*, vol. 93, pp. 892–906, May 2005.

[21] G. E. Lee and D. L. Goldsworthy, "BPA's pacific ac intertie series capacitors: experience, equipment & protection," *IEEE Trans. Power Delivery*, vol. 11, pp. 253-259, Jan. 1996.

[22] T. Van Cutsem, "Voltage instability: phenomena, countermeasures, and analysis methods," *Proc. IEEE*, vol. 88, pp. 208–227, Feb. 2000.

[23] IEEE Power Engineering Society, *FACTS Applications*, Publication 96TP 116-0, IEEE Press, New York, 1996

[24] C. W. Taylor, *Power System Voltage Stability*. EPRI Power System Engineering Series. New York: McGraw Hill, 1994.

[25] K. H. Abdul-Rahman and S. M. Shahidehpour, "Application of fuzzy sets to optimal reactive power planning with security constraints," *IEEE Trans. Power Syst.*, vol. 9, pp. 589-597, May 1994.

[26] J. A. Momoh, S. X. Guo, E. C. Ogbuobiri, and R. Adapa, "The quadratic interior point method solving power system optimization problems," *IEEE Trans. Power Syst*., vol. 9, pp. 1327-1336, Aug. 1994.

[27] K. Y. Lee, X. Bai, and Y. M. Park, "Optimization method for reactive power planning by using a modified simple genetic algorithm," *IEEE Trans. Power Syst*., vol. 10, pp. 1843-1850, Nov. 1995.

[28] W. D. Rosehart, C. A. Canizares, and V. H. Quintana, "Effect of detailed power system models in traditional and voltage-stability-constrained optimal power flow problems," *IEEE Trans. Power Syst*., vol. 18, pp.27-35, Feb. 2003.

[29] O. O. Obadina and G. J. Berg, "Var planning for power system security," *IEEE Trans. Power Syst*., vol. 4, pp. 677-686, May 1989.

[30] W. Xu, Y. Mansour and P. G. Harrington, "Planning methodologies for voltage stability limited power systems," *Electrical Power and Energy Systems*, vol. 15, pp. 221-228, Aug. 1993.

[31] Y. Mansour, W. Xu, F. Alvarado, and C. Rinzin "SVC placement using critical modes of voltage instability", *IEEE Trans. Power Syst.*, vol. 9, pp. 757-763, May 1994.

[32] V. Ajjarapu, P. L. Lau, and S. Battula, "An optimal reactive power planning strategy against voltage collapse", *IEEE Trans. Power Syst.*, vol. 9, pp. 906-917, May 1994.

[33] T. J. Overbye, "Computation of a practical method to restore power flow solvability", *IEEE Trans. Power Syst.*, vol. 10, pp. 280-287, Feb. 1995.

[34] Y. L. Chen, "Weak bus oriented reactive power planning for system security," *IEE Proc. – Gener. Transm. Distrib.*, vol. 143, pp. 541-545, Nov. 1996.

[35] S. Granville, J. C. O. Mello, and A. C. G. Melo, "Application of interior point methods to power flow unsolvability," *IEEE Trans. Power Syst*., vol. 11, pp. 1096-1103, May 1996.

[36] A. J. Wood and B. F. Wollenberg, *Power Generation Operation and Control*, 2nd ed. New York: John Wiley & Sons, Inc., 1996.

[37] C. S. Chang and J. S. Huang, "Optimal multiobjective SVC planning for voltage stability enhancement," *IEE Proc. – Gener. Transm. Distrib.*, vol. 145, pp. 203-209, Mar. 1998.

[38] E. Vaahedi, Y. Mansour, D. Sun, J. Tamby, and W. Li , "Large scale voltage stability constrained optimal VAR planning and voltage stability applications using existing OPF/optimal VAR planning tools," *IEEE Trans. Power Syst*., vol. 14, pp. 65-74, Feb. 1999.

[39] Z. Feng and V. Ajjarapu, "A comprehensive approach for preventive and corrective

control to mitigate voltage collapse", *IEEE Trans. Power Syst*., Vol. 15, pp. 791-797, May 2000.

[40] N. Yorino, E. E. El-Araby, H. Sasaki and S. Harada, "A new formulation for FACTS allocation for security enhancement against voltage collapse", *IEEE Trans. Power Syst*., Vol 18, pp. 3-10, Feb., 2003.

[41] V. Donde and I. A. Hiskens, "Dynamic performance assessment: grazing and related phenomena," *IEEE Trans. Power Syst*., vol. 20, pp. 1967-1975, Nov. 2005.

[42] "Planning against voltage collapse," Electra, vol. 111, pp. 55-75, 1987.

[43] P. Pourbeik, R. J. Koessler, and B. Ray, "Addressing voltage stability related reliability challenges of San Francisco by area with a comprehensive reactive analysis," in *Proc. of the IEEE Power Engineering Society General Meeting*, Jul. 2003, pp. 2634-2639.

[44] P. Pourbeik, R. J. Koessler, W. Quaintance and W. Wong, "Performing comprehensive voltage stability studies for the determination of optimal location, size and type of reactive compensation," in *Proc. of the IEEE Power Engineering Society General Meeting*, Jun. 2006.

[45] V. S. Kolluri and S. Mandal, "Determining reactive power requirements in the southern part of the Entergy system for improving voltage security – a case study," *in Proc. of the IEEE Power Engineering Society General Meeting*, Jun. 2006.

[46] I. Dobson and L. Lu, "Computing an optimal direction in control space to avoid saddle node bifurcation and voltage collapse in electrical power systems," *IEEE Trans. Automatic Control*, vol. 37, pp. 1616-1620, Oct. 1992.

[47] S. Greene, I. Dobson, and F. L. Alvarado, "Sensitivity of the loading margin to voltage collapse with respect to arbitrary parameters," *IEEE Trans. Power Syst*., vol. 11, pp. 845-850, May 1996.

[48]S. Greene, I. Dobson, and F. L. Alvarado, "Contingency ranking for voltage collapse via sensitivities from a single nose curve," *IEEE Trans. Power Syst*., vol. 14, pp. 232-240, Feb. 1999.

[49] B. Long and V. Ajjarapu, "The sparse formulation of ISPS and its application to voltage stability margin sensitivity and estimation," *IEEE Trans. Power Syst*., vol. 14, pp. 944-951, Aug. 1999.

[50] S. Greene, I. Dobson, and F. L. Alvarado, "Sensitivity of transfer capability margins with a fast formula," *IEEE Trans. Power Syst*., vol. 17, pp. 34-40, Feb. 2002.

[51] I. Dobson and L. Lu, "Voltage collapse precipitated by the immediate change in stability when generator reactive power limits are encountered," *IEEE Trans. Circuits Syst*., vol. 39, pp.

762-766, Sept. 1992.

[52] V. Ajjarapu and C. Christy, “The continuation power flow: a tool for steady state voltage stability analysis,” *IEEE Trans. Power Syst*., vol. 7, pp. 416-423, Feb. 1992.

[53] C. A. Canizares and F. L. Alvarado, “Point of collapse and continuation methods for large AC/DC systems,” *IEEE Trans. Power Syst*., vol. 8, pp. 1-8, Feb. 1993.

[54] H. D. Chiang, A. J. Flueck, K. S. Shah, and N. Balu, “CPFLOW: a practical tool for tracing power system steady-state stationary behavior due to load and generation vacations,” *IEEE Trans. Power Syst*., vol. 10, pp. 623-634, May 1995.

[55] M. Ni, J. D. McCalley, V. Vittal, S. Greene, C. Ten, V. S. Ganugula, and T. Tayyib, “Software implementation of online risk-based security assessment,” *IEEE Trans. Power Syst*., vol. 18, pp. 1165-1172, Aug. 2003.

[56] P. M. Anderson and A. A. Fouad, *Power System Control and Stability*, 2nd ed. Piscataway, N.J.: IEEE Press; Wiley-Interscience, 2003.

[57] T. J. Overbye. “A power flow measure for unsolvable cases.” *IEEE Trans. Power Syst.*, vol. 9, pp. 1359-1365, Aug. 1994.

[58] Z. Feng, V. Ajjarapu, and B. Long. “Identification of voltage collapse through direct equilibrium tracing.” *IEEE Trans. Power Syst.*, vol. 15, pp. 342-349, Feb. 1998.

[59] Z. Feng, V. Ajjarapu, and D. J. Maratukulam. “A practical minimum load shedding strategy to mitigate voltage collapse.” *IEEE Trans. Power Syst.*, vol. 13, pp. 1285-1291, Nov. 1998.

[60] A. J. Flueck and J. R. Dondeti, “A new continuation power flow tool for investigating the nonlinear effects of transmission branch parameter variations,” *IEEE Trans. Power Syst.*, vol. 15, pp.223-227, Feb. 2000.

[61] P. Kundur, *Power System Stability and Control*. EPRI Power System Engineering Series. McGraw Hill, 1994.

[62] S. L. Richter and R. A. DeCarlo, “Continuation methods: theory and application,” *IEEE Trans. Circuits Syst*., vol. 30, pp. 347–352, Jun. 1983.

[63] J. Zhao, H. D. Chiang, and H. Li, "A new contingency parameterization CPF model and sensitivity method for voltage stability control," in *Proc. of the IEEE Power Engineering Society General Meeting*, pp. 376-382, Jun. 2005.

[64] M. A. Pai, *Energy Function Analysis for Power System Stability*. Boston: Kluwer Academic Publishers, 1989.

[65] E. Vaahedi, Y. Mansour, C. Fuchs, S. Granville, M. L. Latore and H. Hamadanizadeh, "Dynamic security constrained optimal power flow/Var planning," *IEEE Trans. Power Syst*., vol. 16, pp. 38-43, Feb. 2001.

[66] G. L. Nemhauser and L. A. Wolsey, *Integer and Combinatorial Optimization*. New York : Wiley, 1988.

[67] U.S.-Canada Power System Outage Task Force. Final report on the August 14, 2003 blackout in the United States and Canada: Causes and recommendations. [Online]. Available: https://reports.energy.gov/BlackoutFinal-Web.pdf (Date accessed: Mar. 9, 2007).

[68] "Criteria and countermeasures for voltage collapse," Electra, vol. 162, pp. 159-167, 1995.

[69] S. Kolluri, A. Kumar, K. Tinnium and R. Daquila, "Innovative Approach for solving dynamic voltage stability problem on the Entergy system," in *Proc. of the IEEE Power Engineering Society Summer Meeting*, pp. 988-993, Jul. 2002.

[70] V. S. Kolluri, S. Mandal, Douglas Mader, M. Claus and H. Spachtholz, "Application of static var compensator in Entergy system to address voltage stability issues – planning and design considerations," in *Proc. of the IEEE Power Engineering Society Transmission and Distribution Conf*., pp. 1407-1411, May 2006.

[71] P. Pourbeik, A. Bostrom, and B. Ray, "Modeling and application studies for a modern static var system installation," *IEEE Trans. Power Delivery*, vol. 21, pp. 368-377, Jan. 2006.

[72] J. A. Diaz de Leon II and C. W. Taylor, "Understanding and solving short-term voltage stability problems," *in Proc. of the IEEE Power Engineering Society Summer Meeting*, pp. 745-752, Jul. 2002.

[73] I. A. Hiskens, "Power system modeling for inverse problems," *IEEE Trans. Circuits and Systems* I, vol. 51, pp. 539-551, Mar. 2004.

[74] A. van der Schaft and H. Schumacher, *An Introduction to Hybrid Dynamical Systems*. London, U.K.: Springer-Verlag, 2000.

[75] I. A. Hiskens and M. A. Pai, "Trajectory sensitivity analysis of hybrid systems," *IEEE Trans. Circuits and Systems* I, vol. 47, pp. 204-220, Feb. 2000.

[76] P. M. Frank, *Introduction to System Sensitivity Theory*. New York: Academic Press, 1978.

[77] W. F. Feehery, J. E. Tolsma, and P. I. Barton, "Efficient sensitivity analysis of large-scale differential-algebraic systems," *Applied Numerical Mathematics*, vol. 25, pp. 41-54, Oct. 1997.

[78] S. Li, L. Petzold, and W. Zhu, "Sensitivity analysis of differential-algebraic equations: A comparison of methods on a special problem," *Applied Numerical Mathematics*, vol. 32, pp. 161-174, Feb. 2000.